



David Taylor Research Center

Bethesda, Maryland 20084-5000

DTRC/SHD-1335-02 March 1991

Ship Hydromechanics Department

Asymmetric Preswirl Stator Design for U.S. Coast Guard Island Class Patrol Boats

By

Stephen K. Neely
Benjamin Y-H. Chen

DTRC/SHD-1335-02 Asymmetric Preswirl Stator Design for U.S. Coast Guard Island Class Patrol Boats

91-14257



Approved for public release; distribution unlimited.

91 10 28 057

MAJOR DTRC TECHNICAL COMPONENTS

CODE 011 DIRECTOR OF TECHNOLOGY, PLANS AND ASSESSMENT

12 SHIP SYSTEMS INTEGRATION DEPARTMENT

14 SHIP ELECTROMAGNETIC SIGNATURES DEPARTMENT

15 SHIP HYDROMECHANICS DEPARTMENT

16 AVIATION DEPARTMENT

17 SHIP STRUCTURES AND PROTECTION DEPARTMENT

18 COMPUTATION, MATHEMATICS & LOGISTICS DEPARTMENT

19 SHIP ACOUSTICS DEPARTMENT

27 PROPULSION AND AUXILIARY SYSTEMS DEPARTMENT

28 SHIP MATERIALS ENGINEERING DEPARTMENT

DTRC ISSUES THREE TYPES OF REPORTS:

1. **DTRC reports, a formal series**, contain information of permanent technical value. They carry a consecutive numerical identification regardless of their classification or the originating department.
2. **Departmental reports, a semiformal series**, contain information of a preliminary, temporary, or proprietary nature or of limited interest or significance. They carry a departmental alphanumeric identification.
3. **Technical memoranda, an informal series**, contain technical documentation of limited use and interest. They are primarily working papers intended for internal use. They carry an identifying number which indicates their type and the numerical code of the originating department. Any distribution outside DTRC must be approved by the head of the originating department on a case-by-case basis.

UNCLASSIFIED

SECURITY CLASSIFICATION OF THIS PAGE

REPORT DOCUMENTATION PAGE

1a. REPORT SECURITY CLASSIFICATION UNCLASSIFIED		1b. RESTRICTIVE MARKINGS	
2a. SECURITY CLASSIFICATION		3. DISTRIBUTION/AVAILABILITY OF REPORT Approved for public release; distribution unlimited.	
2b. DECLASSIFICATION/DOWNGRADING SCHEDULE			
4. PERFORMING ORGANIZATION REPORT NUMBER(S) DTRC/SHD-1335-02		5. MONITORING ORGANIZATION REPORT NUMBER(S)	
6a. NAME OF PERFORMING ORGANIZATION David Taylor Research Center	6b. OFFICE SYMBOL (If applicable) Code 1544	7a. NAME OF MONITORING ORGANIZATION	
6c. ADDRESS (City, State, and ZIP Code) Bethesda, MD 20084		7b. ADDRESS (CITY, STATE, AND ZIP CODE)	
8a. NAME OF FUNDING/SPONSORING ORGANIZATION U. S. Coast Guard Research & Development Center	8b. OFFICE SYMBOL (If applicable) CGR&DC 166	9. PROCUREMENT INSTRUMENT IDENTIFICATION NUMBER	
8c. ADDRESS (City, State, and ZIP code) Avery Point Groton, CT 06340		10. SOURCE OF FUNDING NUMBERS	
		PROGRAM ELEMENT NO. 70098	TASK NO. 30227
		TASK NO. 1-1522-830	WORK UNIT ACCESSION NO. 509300
11. TITLE (Include Security Classification) Asymmetric Preswirl Stator Design for U.S. Coast Guard Island Class Patrol Boats			
12. PERSONAL AUTHOR(S) Stephen K. Neely and Benjamin Y-H. Chen			
13a. TYPE OF REPORT Final	13b. TIME COVERED FROM _____ TO _____	14. DATE OF REPORT (Year, Month, Day) 1991, March	15. PAGE COUNT 37
16. SUPPLEMENTARY NOTATION			
17. COSATI CODES		18. SUBJECT TERMS (CONTINUE ON REVERSE IF NECESSARY AND IDENTIFY BY BLOCK NUMBER)	
FIELD	GROUP	SUB-GROUP	
19. ABSTRACT (Continue on reverse if necessary and identify by block number) This report presents the design of an asymmetric preswirl stator for the U.S. Coast Guard Island Class patrol boats. The purpose of the stator is to eliminate a cavitation erosion problem for the propellers. The methods used to analyze the existing propeller and design the asymmetric stator employed extensions to the conventional lifting-line and lifting-surface techniques. The use of a non-axisymmetric lifting line program made it possible to determine the configuration and load distribution which best reduced the likelihood of cavitation erosion. A lifting surface program written specifically for non-axisymmetric stators was used to determine the design geometry. The two dimensional cavitation buckets with corrections for three dimensional effects were used for prediction of blade surface cavitation inception. Also, a panel method was used for prediction of chordwise pressure distributions in a quasi-steady manner. The predicted cavitation inception at the radius of the erosion was increased by 3.5 to 5.5 knots; however, cavitation was not quite eliminated at the full power condition. No significant effect on powering was predicted.			
20. DISTRIBUTION/AVAILABILITY OF ABSTRACT <input type="checkbox"/> UNCLASSIFIED/UNLIMITED <input checked="" type="checkbox"/> SAME AS RPT. <input type="checkbox"/> DTIC USERS		21. ABSTRACT SECURITY CLASSIFICATION UNCLASSIFIED	
22a. NAME OF RESPONSIBLE INDIVIDUAL Stephen K. Neely		22b. TELEPHONE (Include Area Code) (301)227-1453	22c. OFFICE SYMBOL Code 1544

TABLE OF CONTENTS

	Page
NOMENCLATURE	v
ABSTRACT	1
ADMINISTRATIVE INFORMATION	1
INTRODUCTION	1
DESIGN CONSTRAINTS	2
WAKE PREDICTION	2
EXISTING PROPELLER REPRODUCTION	3
ASYMMETRIC STATOR DESIGN	4
Basic Configuration	4
Load Distribution	5
Blade Geometry	6
RESULTS AND DISCUSSION	7
REFERENCES	31

FIGURES

	Page
1. Erosion Damage	9
2. USCG Island Class Patrol Boat, Stern Arrangement	10
3. Nominal Wake Estimate	11
4. Mean Nominal and Effective Wakes	11
5. Existing Propeller Powering Performance	12
6. Cavitation Bucket With Original Inflow -- 0.3R	13
7. Chordwise Pressure Distribution -- 0.325R	14
8. Chordwise Pressure Distribution -- 0.722R	15
9. Stator Configuration	16
10. Stator Design Load Distribution	17
11. Modified Tangential Wake in the Propeller Plane	18
12. Stator Chord and Thickness	19
13. Section Maximum Thickness and Trailing Edge Thickness	19
14. Stator Design Parameters	20
15. Stator Camber Distribution	21
16. Stator Pitch Distribution	21
17. Expanded Hub	22

FIGURES (Continued)

	Page
18. Stator Blade Sections	23
19. Cavitation Bucket with Modified Inflow -- 0.3R	24
20. Modified Chordwise Pressure Distribution -- 0.325R	25

TABLES

1. Stator Design Geometry (D=20 in.)	26
2. Stator Design Geometry (in inches)	27
3. Blade Pitch Settings	28
4. Net Stator Forces (per shaft)	28
5. Cavitation Inception Speeds (knots)	29

NOMENCLATURE

c	Chord length
C_L	Lift coefficient: $C_L = \frac{L}{\frac{1}{2}\rho c V_{REL}^2}$
C_p	Pressure coefficient, normalized by V_{REL} : $C_p = \frac{p - p_\infty}{\frac{1}{2}\rho V_{REL}^2}$
C_{pMIN}	Minimum C_p : $C_{pMIN} = \frac{p_{MIN} - p_\infty}{\frac{1}{2}\rho V_{REL}^2}$
C_{ps}	Pressure coefficient, normalized by V_S : $C_{ps} = \frac{p - p_\infty}{\frac{1}{2}\rho V_S^2}$
D	Diameter
D_S	Stator diameter
f	Maximum camber
G	Non-dimensional circulation: $G = \frac{\Gamma}{2\pi R V_S}$
J_S	Advance coefficient: $J_S = \frac{V_S}{nD}$
K_Q	Torque coefficient: $K_Q = \frac{Q}{\rho n^2 D^5}$
L	Lift
n	Shaft speed, revolutions per second: $n = RPM/60$
p	Local pressure
p_{MIN}	Minimum pressure
p_∞	Ambient pressure
P_D	Delivered power
r	Local radius
R	Maximum radius
R_S	Stator radius
RPM	Shaft speed, revolutions per minute
t	Thickness
t_{TE}	Trailing edge thickness
V_r	Radial velocity
V_{REL}	Relative velocity
V_S	Ship speed
V_t	Tangential velocity
V_x	Axial velocity

NOMENCLATURE (Continued)

x_R	Total rake	
$1-w_e$	Volumetric mean effective wake	
$1-w_n$	Volumetric mean nominal wake	
$1-w_T$	Thrust identity wake fraction	
ϕ	Pitch angle	
θ_S	Skew	
σ	Cavitation number, normalized by V_{REL} :	$\sigma = \frac{p_\infty - p_v}{\frac{1}{2}\rho V_{REL}^2}$
σ_S	Cavitation number, normalized by V_S :	$\sigma_S = \frac{p_\infty - p_v}{\frac{1}{2}\rho V_{REL}^2}$
ρ	Fluid density	
Γ	Circulation	

ABSTRACT

This report presents the design of an asymmetric preswirl stator for the U.S. Coast Guard Island Class patrol boats. The purpose of the stator is to eliminate a cavitation erosion problem for the propellers. The methods used to analyze the existing propeller and design the asymmetric stator employed extensions to the conventional lifting-line and lifting-surface techniques. The use of a non-axisymmetric lifting line program made it possible to determine the configuration and load distribution which best reduced the likelihood of cavitation erosion. A lifting surface program written specifically for non-axisymmetric stators was used to determine the design geometry. The two dimensional cavitation buckets with corrections for three dimensional effects were used for prediction of blade surface cavitation inception. Also, a panel method was used for prediction of chordwise pressure distributions in a quasi-steady manner. The predicted cavitation inception at the radius of the erosion was increased by 3.5 to 5.5 knots; however, cavitation was not quite eliminated at the full power condition. No significant effect on powering was predicted.

ADMINISTRATIVE INFORMATION

This work was performed by Code 1544 of the David Taylor Research Center (DTRC) and was supported by the U.S. Coast Guard (USCG) under work request 30227. Work was performed under DTRC work unit 1-1522-830.

INTRODUCTION

The propellers on the U.S. Coast Guard 110 ft. Island Class patrol boats have a serious cavitation erosion problem. After a relatively short period of time of operation at the full power condition, deep pits appear at the root of each blade near midchord of the suction surface. In a previous attempt to cure the erosion problem, two holes were drilled near the hub of each blade. However, as shown in Figure 1, erosion still occurs on the propellers with the holes. The erosion problem affects over 100 propellers worth about three million dollars. To protect its investment, the U.S. Coast Guard requested David Taylor Research Center to design a device which would eliminate the erosion problem. After a preliminary study, it was determined that the erosion was caused by leading edge suction side cavitation due to the high angle of attack associated with an inclined shaft. This form of cavitation could be reduced by the installation of an asymmetric stator.

The purpose of this report is to discuss the DTRC design of an asymmetric stator for the U.S. Coast Guard. The following sections describe the approach taken, beginning with design constraints imposed by USCG and prediction of the wake for the existing condition. Given a wake and propeller geometry, reproduction of powering and cavitation for the existing propeller is

described. The design of the stator is then described, followed by the prediction of powering and cavitation for the modified configuration. Finally, conclusions and recommendations are provided.

DESIGN CONSTRAINTS

Design constraints imposed by USCG played an important role in the design of the stator. These constraints, which were imposed to minimize the cost and complication of construction, are listed below.

- Existing propeller cannot be modified.
- Stator is limited to the region of the existing rope guard.
- Each stator blade must have identical geometry (however, each blade may be rotated to obtain the appropriate pitch setting).

The rope guard is a ring located on the hub directly forward of the propeller, as shown in Figure 2. The length of the rope guard, which is only $3\frac{1}{8}$ inches (0.079 m), limits the size and effectiveness of the stator.

WAKE PREDICTION

The nominal wake in the plane of the propeller was necessary for the prediction of cavitation as well as for the design of the stator. However, wake survey data were not available for this boat and it was necessary to estimate the wake based on a previous wake survey for a similar hull form. The Coast Guard boat is 110 feet (33.54 m) long and has a maximum speed of 30 knots. It has an open stern with twin shafts each supported by a single vertical strut. The shafts are inclined downward approximately 11 degrees relative to the hull buttock lines. The U.S. Navy boat R/V Athena was found to have similar features. Athena is 160 feet (48.78 m) long and has a maximum speed of 30 knots. Athena also has an open stern, twin shafts and approximately 11 degrees shaft inclination. Since wake survey data were available for Athena, the predicted wake for the Coast Guard boat was based primarily on the model wake survey for Athena¹. The predicted nominal wake is shown in Figure 3.

The effective wake was also estimated based on model test measurements for the R/V Athena². Propulsion tests indicated a thrust identity wake fraction, $1-w_T$, of approximately 1.0 for Athena. The effective wake for the USCG boat was obtained by simply scaling the nominal wake by a constant such that the volume mean effective wake, $1-w_e$, was equal to 1.0. The mean nominal and effective wakes are shown in Figure 4.

EXISTING PROPELLER REPRODUCTION

The first step in solving the erosion problem was to reproduce the conditions for the existing propeller using propeller analysis tools. First, the delivered power, P_D , at the full power condition was predicted using a lifting surface analysis method developed by Greeley³, extended to include hub boundary effects. The Coast Guard had provided data from ship trials⁴, which included P_D and RPM as a function of ship speed, V_S . The results, shown in Figure 5, showed reasonable agreement between predictions and measurements. Second, the cavitation at the full power condition was predicted using two methods as described in the following paragraphs.

The first procedure used for prediction of cavitation was the traditional "cavitation bucket" method developed by Brockett⁵. This procedure calculates the minimum surface pressure, C_{pMIN} , where

$$C_{pMIN} = \frac{p_{MIN} - p_{\infty}}{1/2\rho V_{REL}^2}, \text{ and}$$

V_{REL} = local relative inflow velocity,

for a 2D airfoil at various steady angles of attack. The result is a cavitation bucket which defines regions for various types of cavitation. The cavitation bucket is fixed for a fixed section geometry. The propeller operating condition is represented by the cavitation index, σ , where

$$\sigma = \frac{p_{\infty} - p_v}{1/2\rho V_{REL}^2},$$

The cavitation index is plotted as a function of angle of attack for a propeller section as it rotates through the unsteady inflow. Points which fall outside of the bucket indicate cavitation over that portion of the propeller rotation. An angle of attack reduction factor is applied to account for steady 3D effects. However, since the flow is assumed quasi-steady, the unsteady effect on pressure and angle of attack is ignored. Cavitation buckets for the USCG boat were calculated for the 30 knot, full power condition. The result for the 0.3R radius, as shown in Figure 6, indicates that when the blade is in the 270° position, the propeller experiences leading edge suction side cavitation. At the 90° position, inception of leading edge pressure side cavitation is evident. There is no indication of back bubble cavitation at 30 knots.

The second method for prediction of cavitation was based on a panel method developed by Lee⁶. Using this method, the propeller blade pressure distribution was determined for the steady flow condition. Hub boundary and steady 3D effects are included. However, the inflow must be considered quasi-steady in order to examine the circumferential variation in angle of attack.

Results are shown in Figure 7 for a single radius near the hub (0.325R) with the blade at 90° and 270°. In this case, the pressure coefficient and the cavitation index are normalized by the ship speed:

$$C_{ps} = \frac{p - p_{\infty}}{1/2 \rho V_S^2}, \text{ and}$$

$$\sigma_s = \frac{p_{\infty} - p_v}{1/2 \rho V_S^2} = 0.925 \text{ (at 30 kts).}$$

This figure indicates leading edge suction side cavitation at 30 knots when the blade is at 270° and leading edge *pressure side* cavitation at 90°. Thus both cavitation prediction methods indicate similar forms of cavitation at the full power condition. The pressure distribution at the 0.722R, shown in Figure 8, is also provided at 90° and 270° to show the greater extent of cavitation at larger radii. (In particular, note that *suction side* cavitation occurs at both 90° and 270°. Since the *minimum* angle of attack occurs at 90°, this implies that this cavitation occurs for the full revolution of the blade.)

Since back bubble cavitation was not predicted in either case, it was concluded that leading edge suction side cavitation was the cause of the erosion. Although this cavitation was predicted to be much more extensive at larger radii, the erosion occurred only near the hub. The most promising way to eliminate the erosion was to eliminate the cavitation. Since leading edge cavitation was caused by excessive angle of attack, a preswirl stator was designed to reduce the circumferential variation in tangential velocity.

ASYMMETRIC STATOR DESIGN

This section presents the rationale used in the design of the asymmetric preswirl stator. The basic configuration is first explained, which includes the selection of diameter, number of blades, and location of blades. The spanwise distribution of loading is then explained and its effect on the downstream velocity distribution. Finally, selection of the blade geometry, which includes spanwise distribution of chord, thickness, camber, and pitch, is explained.

Basic Configuration

The stator diameter was selected to be large enough such that the stator could adequately affect the inflow to the propeller in the region of the erosion. The erosion occurred on the propeller near the 0.3R radius, which was approximately 2.5 inches away from the hub. Thus, a 5.0 inch span was selected which, given a 10 inch hub diameter, led to a 20 inch stator diameter. A larger

diameter would have led to an unnecessary amount of drag and a higher stress level at the root of the blades.

The selection of blade number and blade locations was based on a variety of reasons. Since propeller leading edge suction side cavitation was a problem in the 270° region, stator blades were necessary in this region to eliminate the existing erosion problem. These blades needed to turn the flow downward which required that they be lifting upward. This configuration would have been adequate. However, upwash from these blades occurred in the 90° region which aggravated propeller leading edge pressure side cavitation. This form of cavitation is known to be more violent than leading edge suction side cavitation and erosion on the pressure side may occur. To prevent leading edge pressure side cavitation, stator blades were also required in the 90° region. Since these blades must also lift upward, the camber must be in the reverse direction of the blades at 270° . Thus at least two blade geometries were required, which violated the design requirement of only one blade geometry. It was quickly realized, however, that a mirror image geometry would be necessary for the port stator and there were actually two blade geometries to work with. Thus the blades in the 90° region were designed to be a mirror image of those in the 270° region. In order to eliminate possible cavitation due to the strut viscous effect, a blade was also positioned at 0° . The selected load distribution, which is discussed later, had a finite value at the hub. Since this can lead to a strong hub vortex and a drag penalty, a blade was also positioned at 180° to cancel the swirl of the blade at 0° .

As stated in the design constraints, the stator was limited to the region of the existing rope guard. This rope guard was only $3\frac{1}{8}$ inches long. This restriction limited the chord length of the stator blades which in turn limited the amount of load each blade could carry. In order to produce enough swirl, the number of blades was maximized. For ease of construction, the minimum blade spacing was selected to be 30° . For these reasons, four blades were positioned around 270° and 90° . This basic configuration is shown in Figure 9.

Load Distribution

The shape of the spanwise circulation distribution, G , greatly affected the stator induced velocity in the plane of the propeller. The magnitude of the loading was selected in conjunction with the blade geometry and is discussed later. A lifting line method developed by Kerwin⁷, which was capable of computing forces and field point velocities for an asymmetric stator, was used for the selection of load distribution. A finite hub loading with a significant extent of zero slope near the hub led to the most desirable distribution of velocity downstream. This distribution is shown in Figure 10. Since there was no slope near the hub, there was no shed vorticity in this region. The load near the tip was reduced in order to prevent tip vortex cavitation. The resulting predicted distribution of tangential velocity in the plane of the propeller is shown for three radii in

Figure 11. The wake at the $0.759R_s$ ($0.306R$) as shown in Figure 11b, which represents the modified wake at the radius where the erosion occurred, indicates a 40% reduction of the tangential velocity at 90° and 270° .

Blade Geometry

The chord length was maximized in order to achieve the greatest amount of loading. Given a hub length of $3\frac{1}{8}$ inches, the root chord of the blade was selected to be 2.9 inches. The lift coefficient, C_L , is related to the chord length, c , and the circulation, Γ , as follows:

$$C_L = \frac{L}{\frac{1}{2}\rho c V_{REL}^2} = \frac{4\pi G}{(c/D)(V_{REL}/V_S)}$$

where $G = \frac{\Gamma}{2\pi R V_S}$ and $L = \rho V_{REL} \Gamma$.

In order to provide a margin against stall, the lift coefficient was selected to be no more than 0.5. Since the load distribution was constant near the hub and the relative velocity was nearly constant, the chord was held constant near the hub in order to maintain a C_L equal to 0.5. The chord was rounded down to 1.5 inches at the tip where the load distribution goes to zero. A finite chord was maintained at the tip in order to help prevent tip vortex cavitation. The distribution of chord and thickness are provided in Figure 12.

The thickness, t , was selected to be large enough to provide strength while not inducing back bubble cavitation. The following approximate formula based on the cavitation buckets for a NACA 16 section was used to check the margin against back bubble cavitation:

$$-C_{P_{MIN}} \approx 2.28*(t/c) + 0.56*C_L$$

The ratio $C_{P_{MIN}}/\sigma$ and C_L are shown in Figure 14a. The maximum stress was calculated based on beam theory. The stress for the full power steady ahead condition is shown in Figure 14b. The standard practice for maximum allowable stress for a propeller is 12,500 psi (for nickel-aluminum-bronze). The maximum stress at the hub of the stator was only 2,800 psi, well below the standard limit. To increase the robustness of the trailing edge, a parabolic thickness addition was applied to the standard airfoil sections aft of midchord. The total trailing edge thickness, t_{TE} , as shown in Figure 13, was maintained greater than or equal to $\frac{1}{32}$ of an inch.

The camber, f , and pitch, ϕ , were determined using lifting surface design methods. Since no lifting surface code was available for asymmetric stator design, blades in the 270° region were simulated by computing the lifting surface geometry for an axisymmetric 12 bladed stator. For this computation, the lifting surface design method by Wang⁸ with extensions for hub boundary effects

was used. The results are shown in Figure 15 for camber. There was essentially no lifting surface correction for pitch.

From the lifting line analysis, the hydrodynamic pitch for each blade was determined. However, the design requirements stated that only a single blade geometry could be designed. Since the load distribution for each blade was the same, the distribution of pitch for each blade was similar. Thus it was expected that if the average pitch distribution for all the blades was used, the original design load distribution could be nearly sustained. The average design pitch distribution is shown in Figure 16. Using the lifting surface analysis method for asymmetric stators described by Hsin⁹, each blade was then rotated in an attempt to obtain the design loading. This required a simultaneous iteration of the pitch of each blade until the original design loading was obtained. The pitch setting and the hub section for each blade is illustrated in Figure 17 on an expanded hub surface. For additional appreciation of the design geometry, the plot of blade sections is provided in Figure 18. Tabulated geometry is provided in Tables 1 through 3.

A note on final geometry is necessary since the blade pitch settings were changed during model testing. The blade pitch settings were adjusted for the model test since the shaft/strut assembly in the water tunnel was fixed at 9.25° relative to the flow, while according to the *predicted* wake (based on the R/V Athena, as described in this report) the actual inflow to the propeller is inclined approximately 11.5° . Thus, in order for the stator blades to achieve the design loading, the blades were rotated appropriately.

The blade pitch settings for full scale were selected to be the same as model scale. The reasoning behind this decision was two-fold. First, based on past experience with inclined shaft sterns, some people felt that the model test configuration represented a more appropriate wake than the predicted wake. Second, if the *predicted* wake is correct, then using the model scale pitch would lead to a stator blade loading higher than design. An error in this direction is preferred since the propeller cavitation is more likely to be reduced if the stator loading is too high rather than too low. The pitch settings selected for full scale are listed in Table 3.

RESULTS AND DISCUSSION

The effect of the stator on powering and cavitation performance is now presented. From the lifting line analysis, the net forces from the stator were computed. The longitudinal, vertical, and lateral forces are listed in Table 4. The longitudinal drag of 11 lbs. per shaft is negligible compared to the 20,000+ lbs. of thrust each propeller produces. Thus no significant effect on powering is expected.

The modified flow behind the stator was used to determine the impact on cavitation performance of the propeller. The two cavitation prediction methods were repeated for the new condition. The cavitation bucket, shown in Figure 19, indicates that leading edge suction side

cavitation is at inception at 270° . While the panel method, shown in Figure 20, shows a reduction of the suction peak, cavitation is still evident. At 90° the cavitation bucket showed a large margin against pressure side cavitation while the panel method shows cavitation inception. The cavitation inception speed was determined for both methods for various types of cavitation at the $0.3R$ radius and is shown in Table 5. The panel method predicts lower inception speeds in all cases. The principal result is the increase in leading edge suction side cavitation inception speed at the $0.3R$ radius of the propeller of approximately 3.5 to 5.5 knots.

The asymmetric preswirl stator as designed will significantly reduce the cavitation at the hub of the propeller. Thus the goal of the design, which was to eliminate the cavitation erosion, appears to be achieved. Since the prediction of cavitation erosion is beyond the state-of-the-art, the success of the design can only be determined experimentally. Cavitation tests have been performed and comparison of computations versus measurements of stator/propeller performance will be reported separately. It is recommended that the design requirement of limiting the stator to the region of the rope guard be lifted, and a larger stator be designed which could carry a greater load such that cavitation at the hub of the propeller is eliminated.

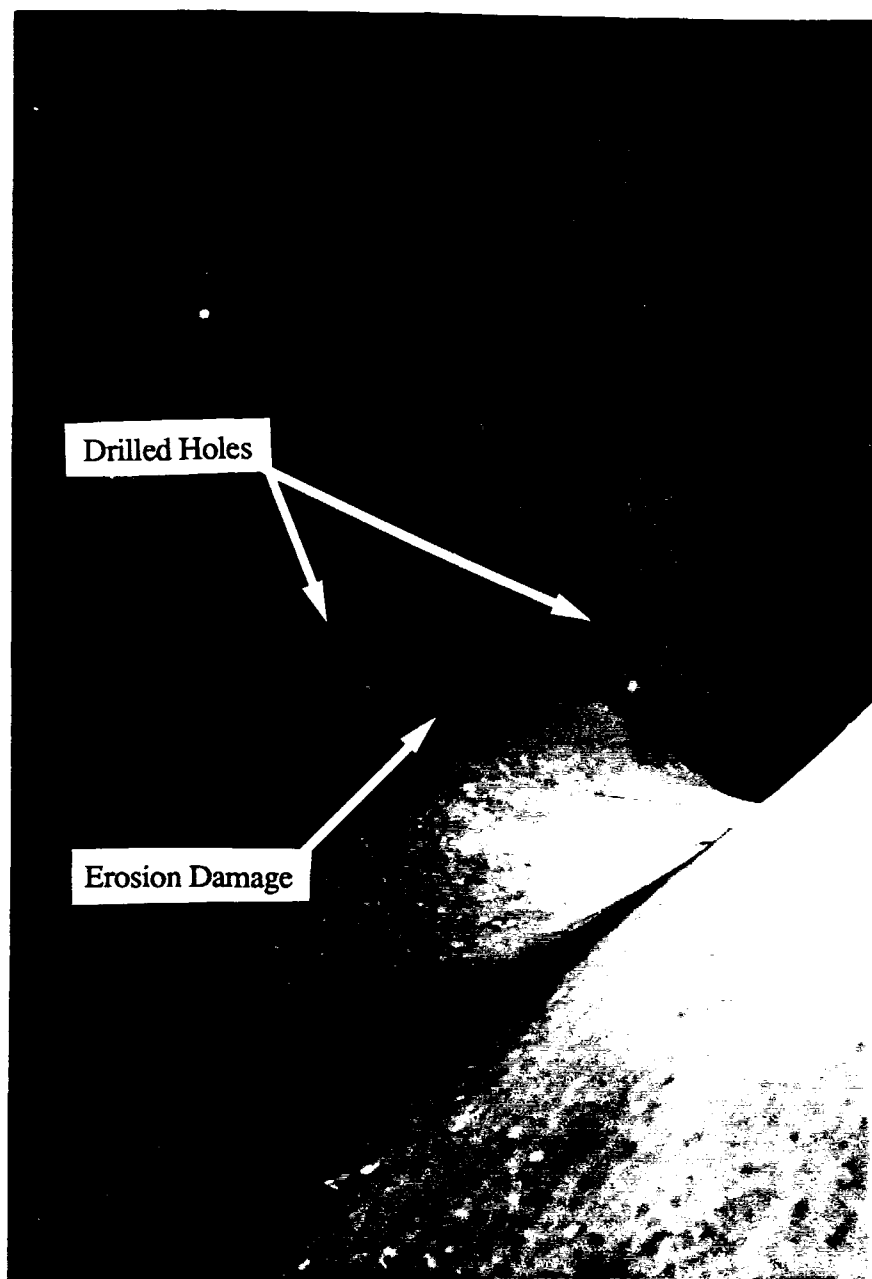


Figure 1. Erosion Damage

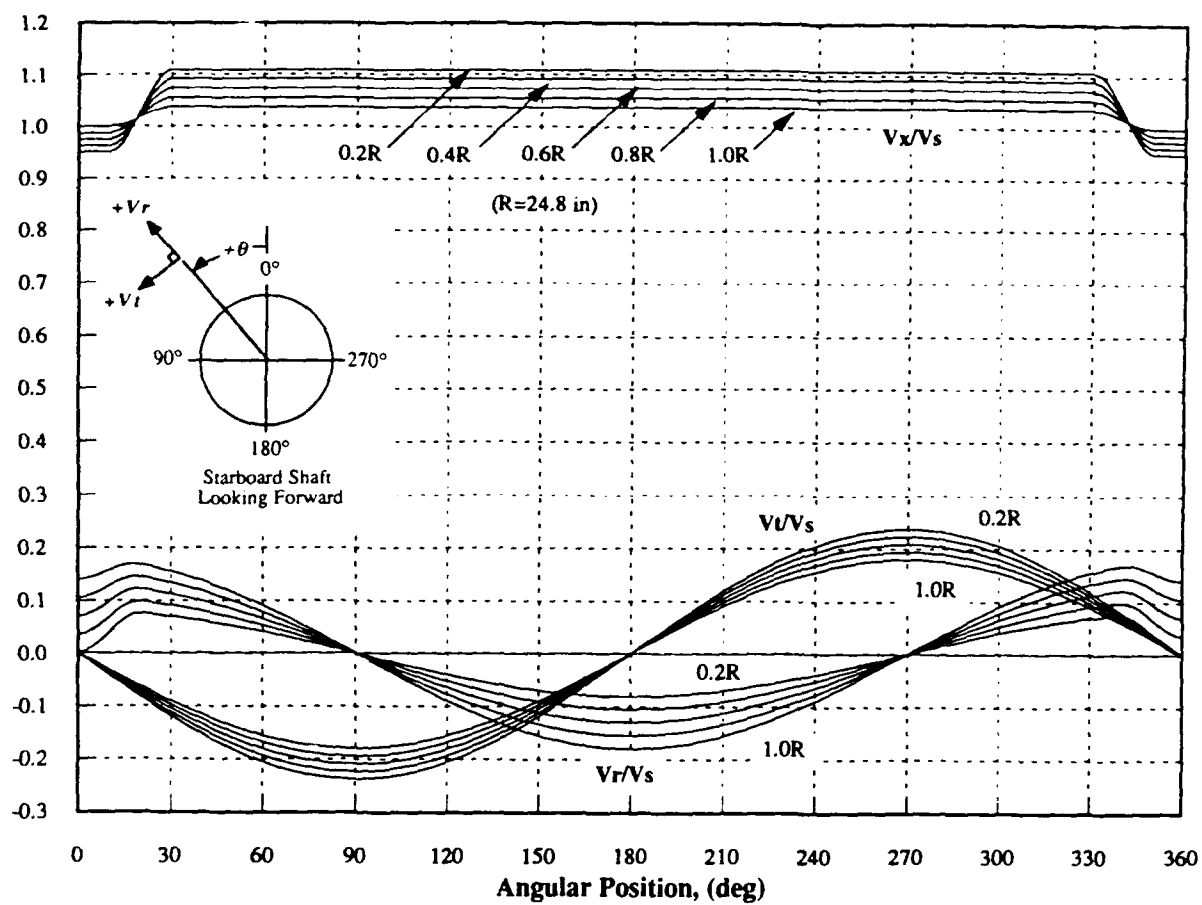


Figure 3. Nominal Wake Estimate

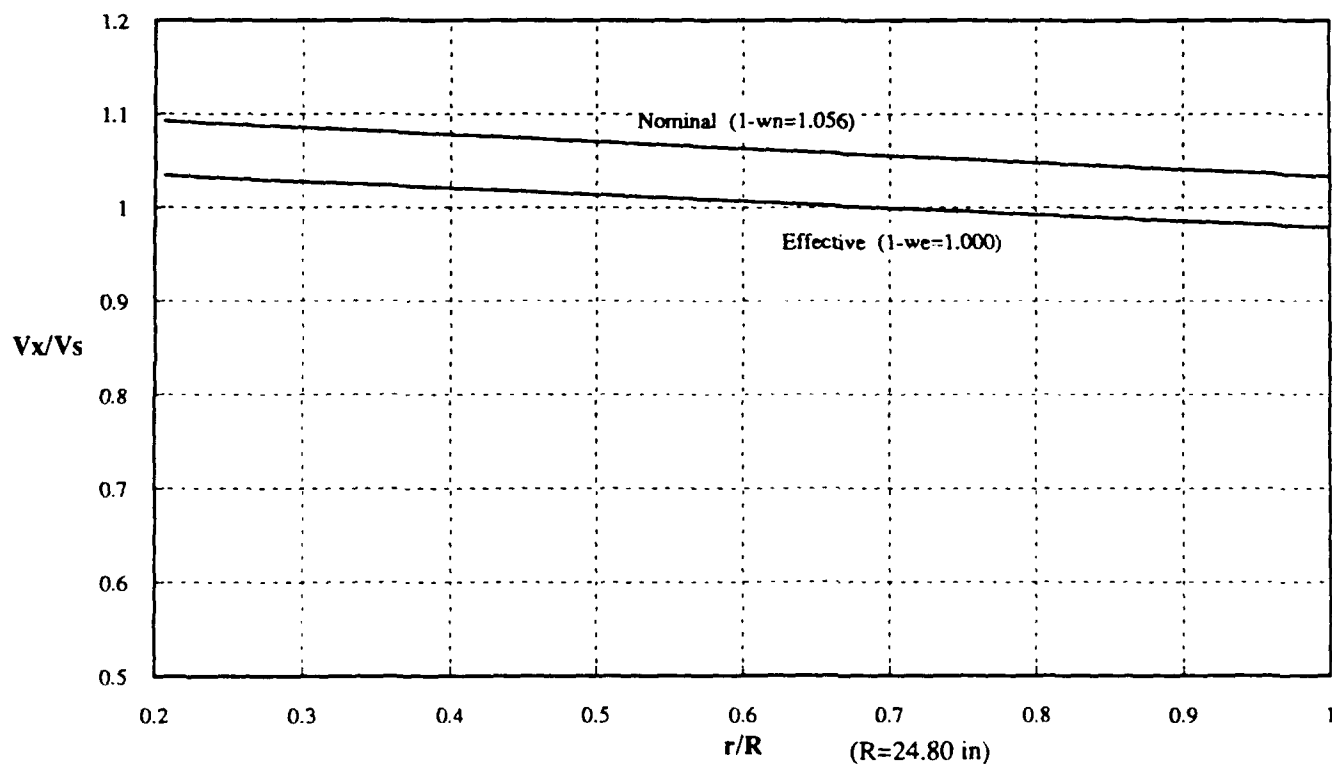


Figure 4. Mean Nominal and Effective Wakes

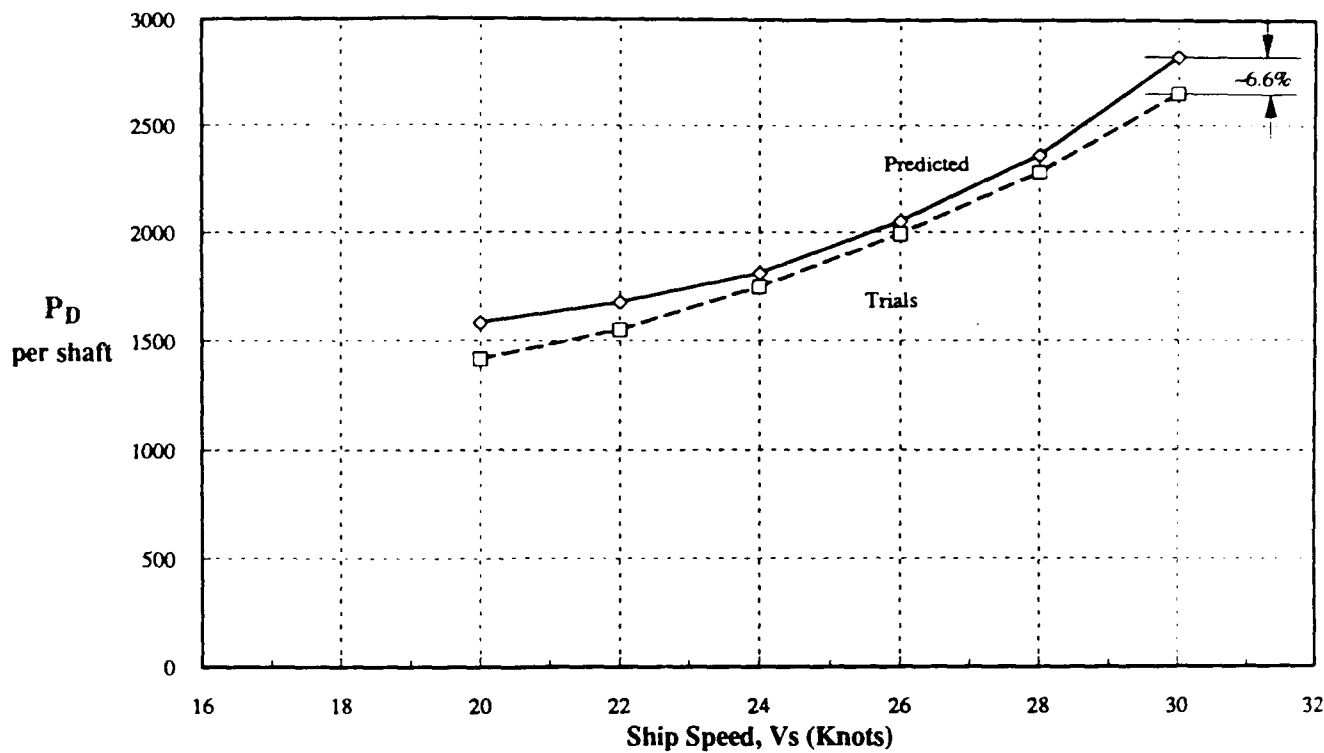


Figure 5a. Delivered Power vs. Ship Speed

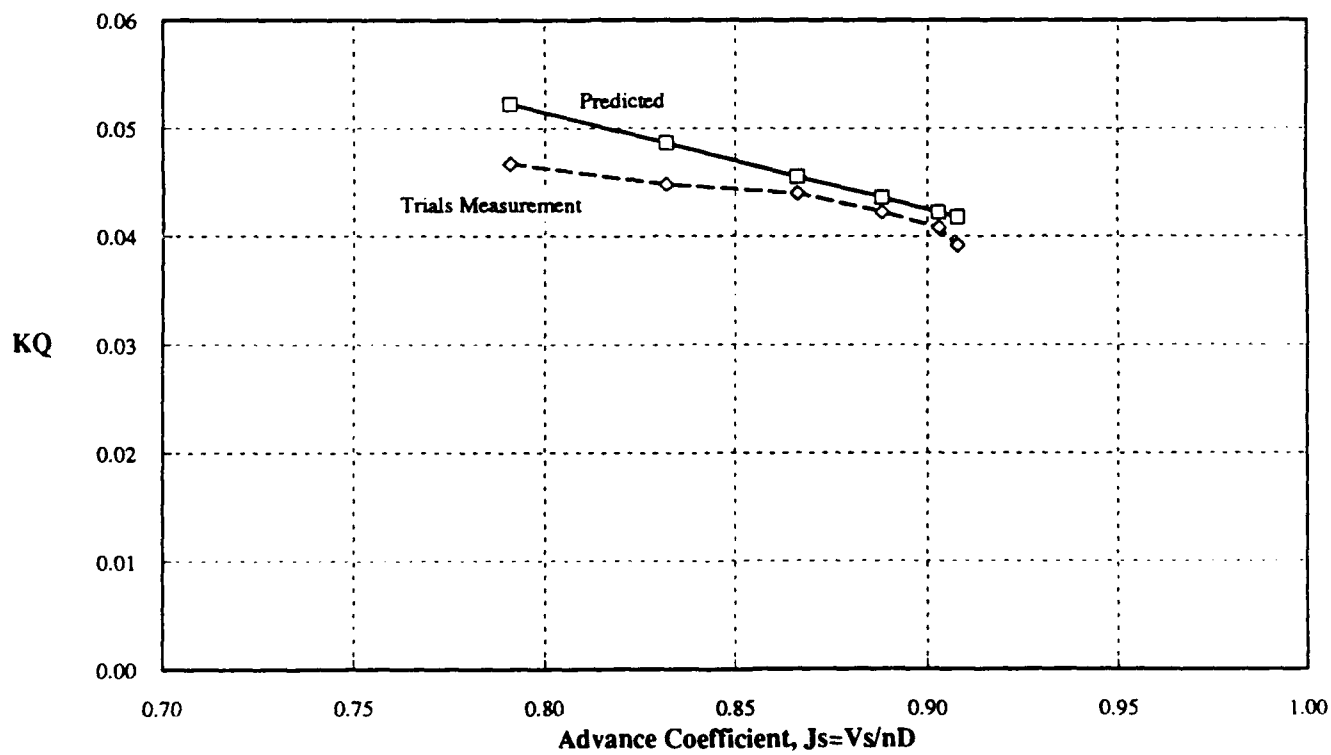


Figure 5b. Torque Coefficient vs. Advance Coefficient

Figure 5. Existing Propeller Powering Performance

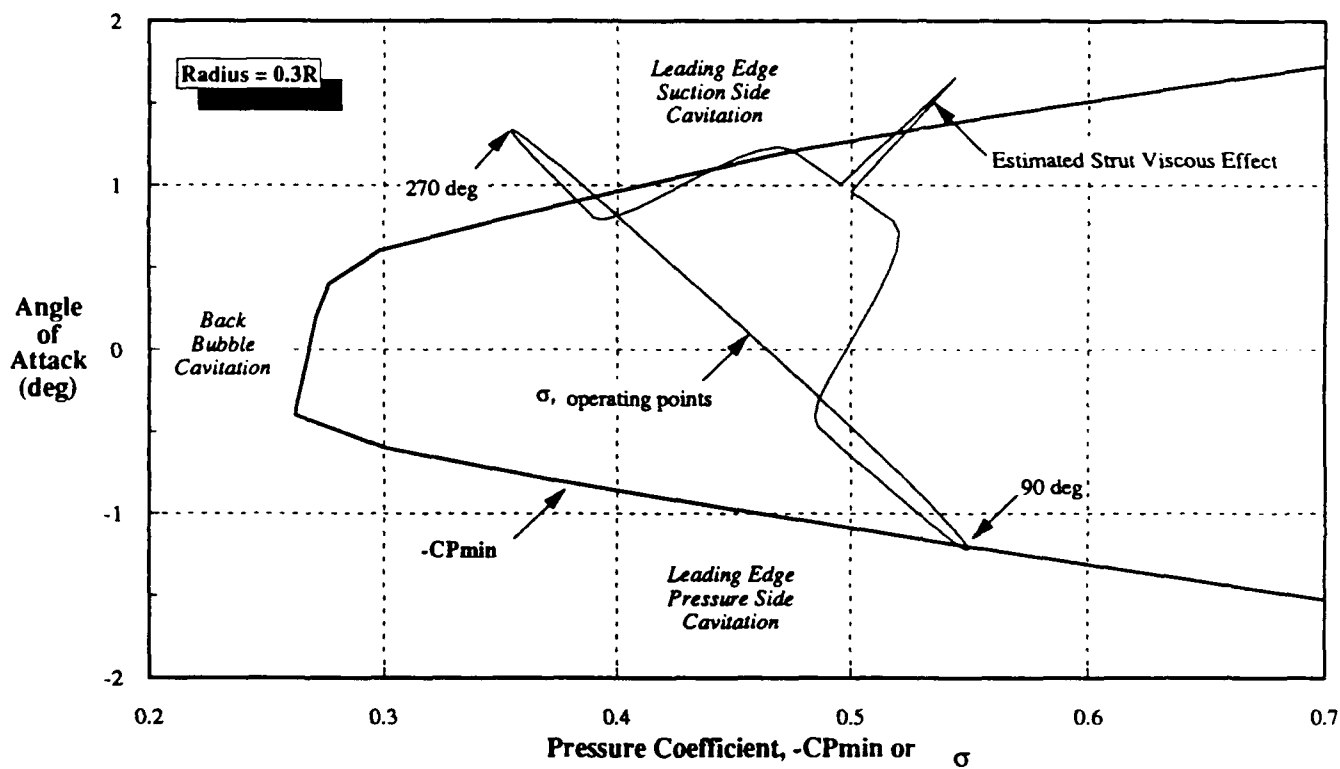


Figure 6. Cavitation Bucket With Original Inflow -- $0.3R$

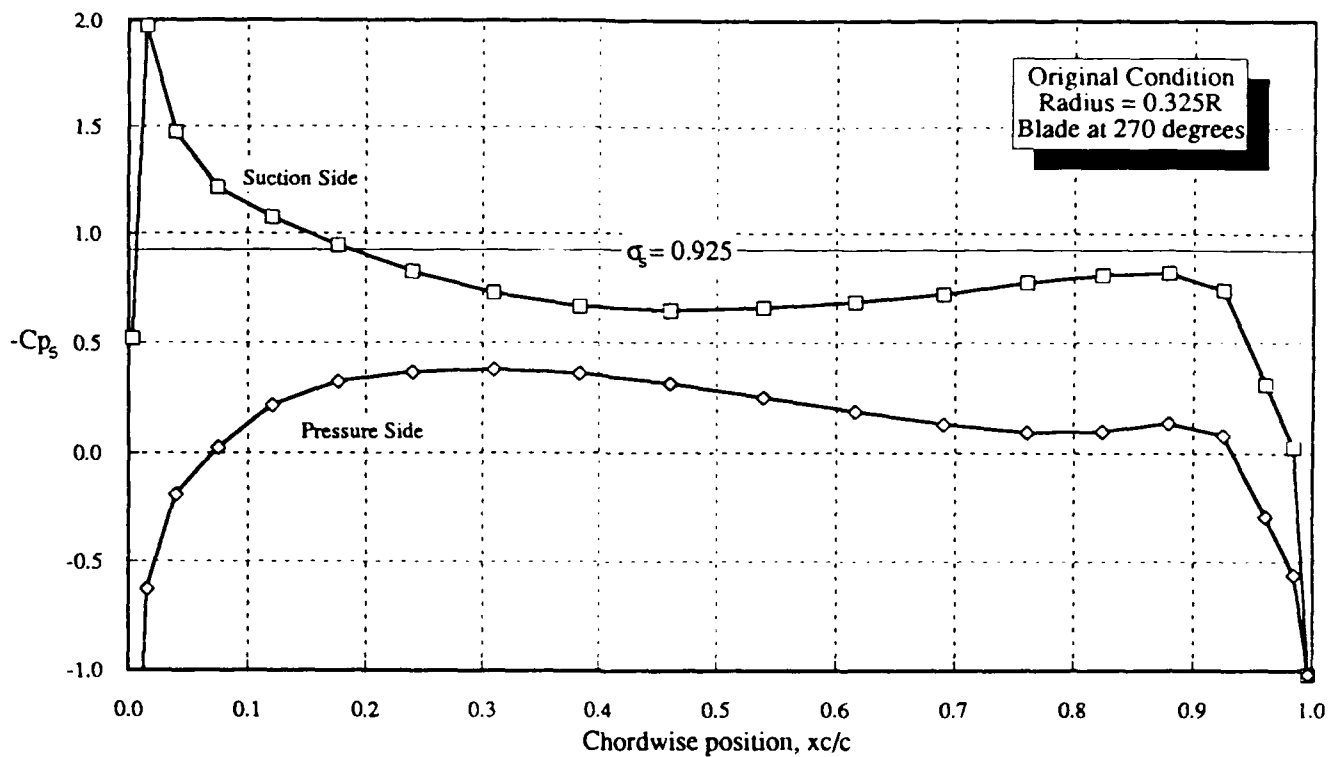


Figure 7a. Blade at 270 degrees

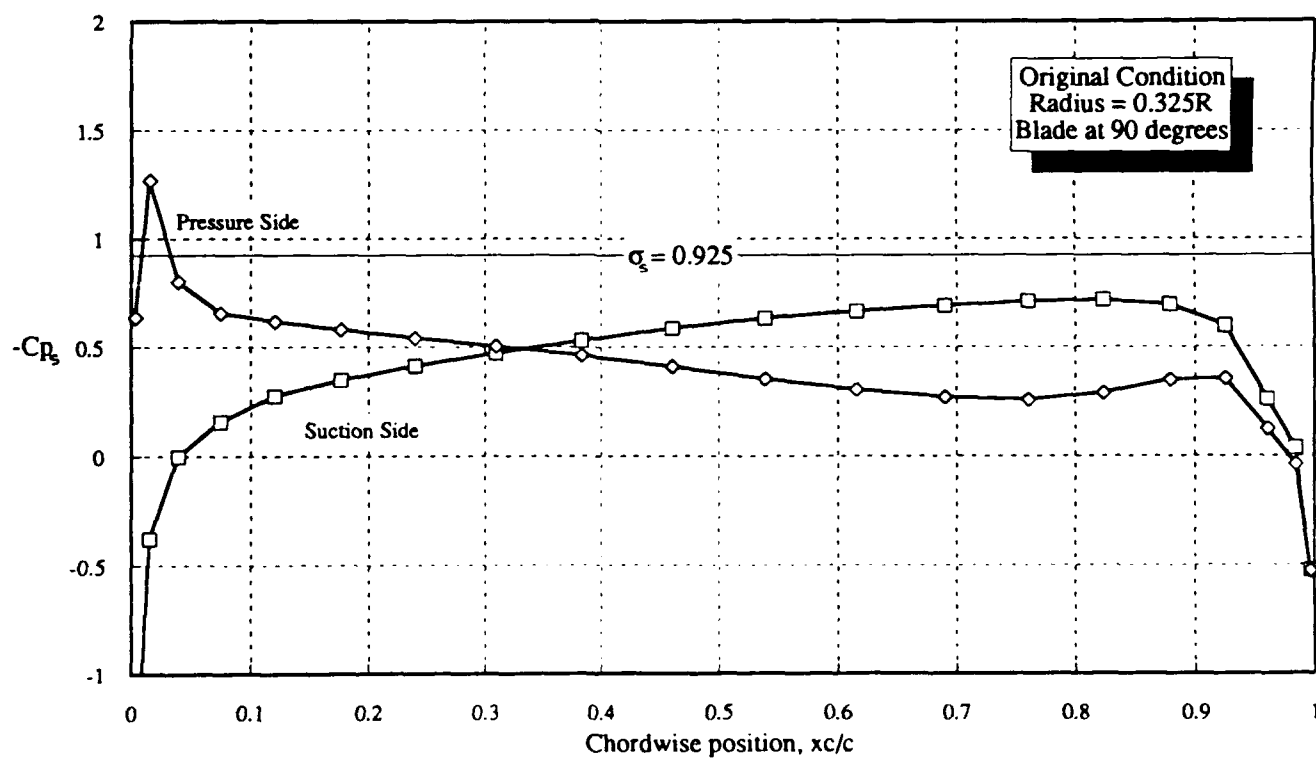


Figure 7b. Blade at 90 degrees

Figure 7. Chordwise Pressure Distribution -- 0.325R

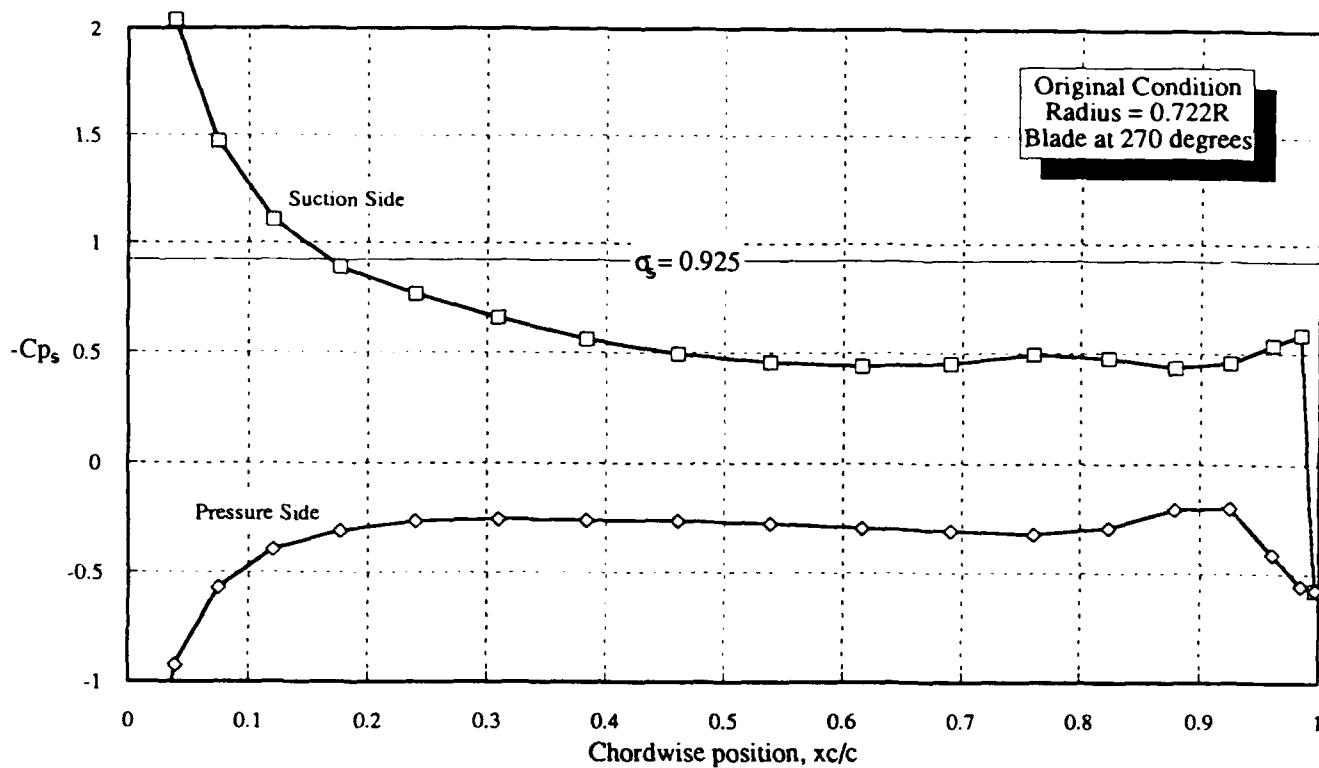


Figure 8a. Blade at 270 degrees

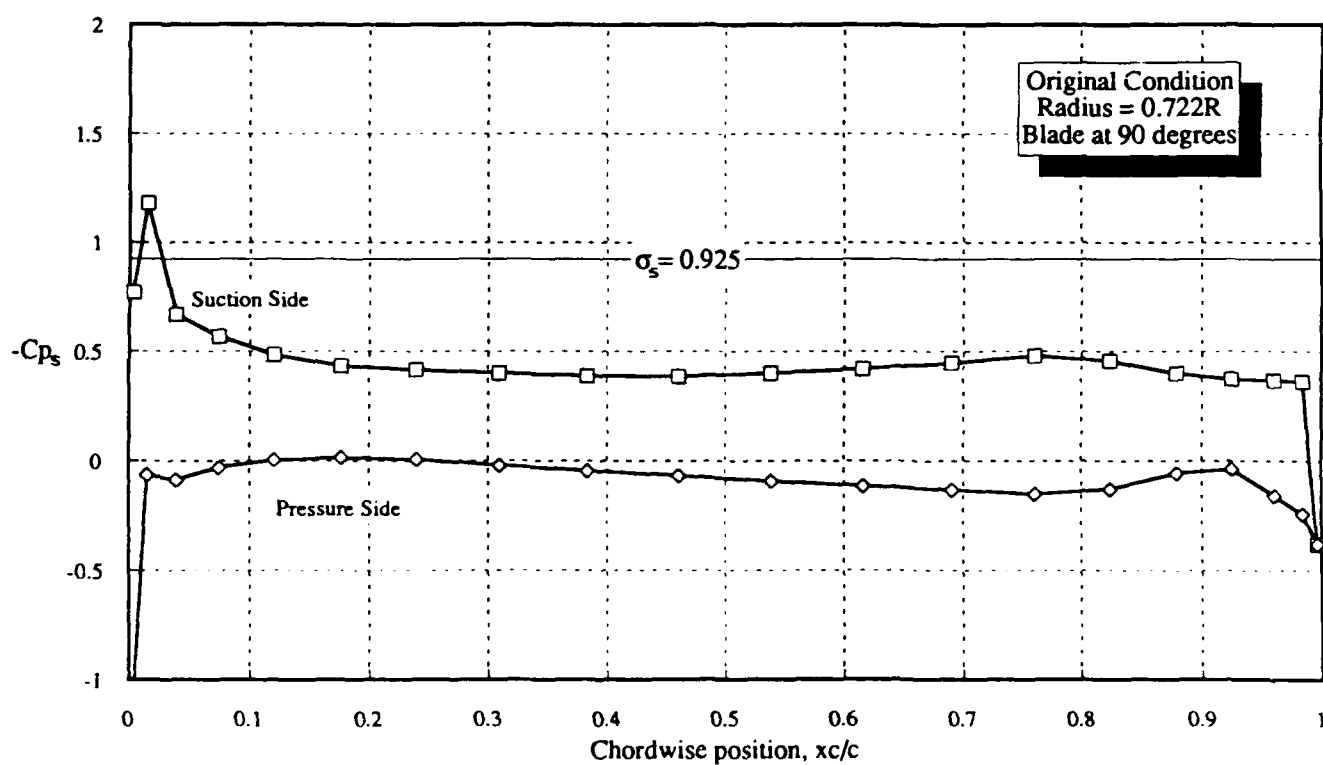


Figure 8b. Blade at 90 degrees

Figure 8. Chordwise Pressure Distribution -- 0.722R

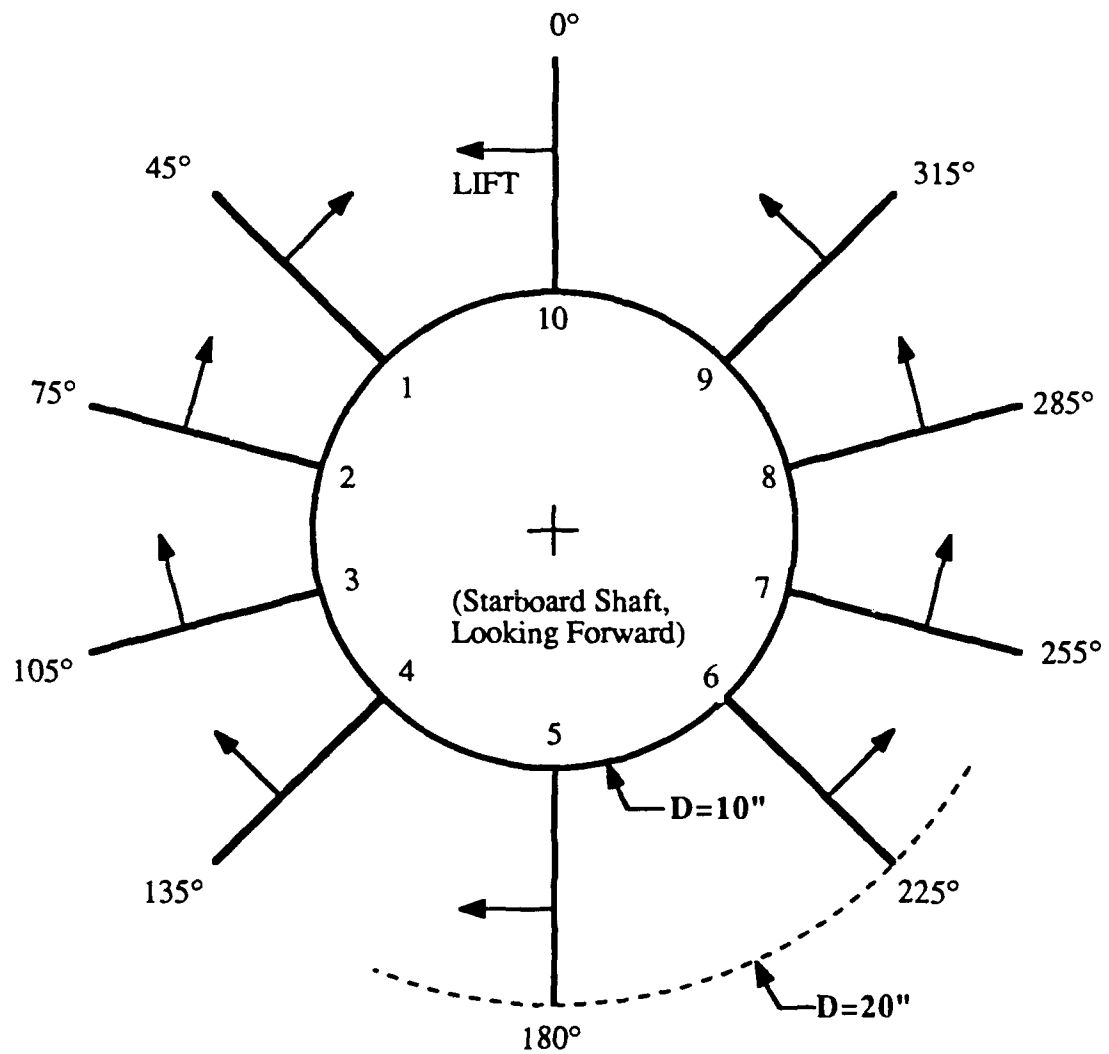


Figure 9. Stator Configuration

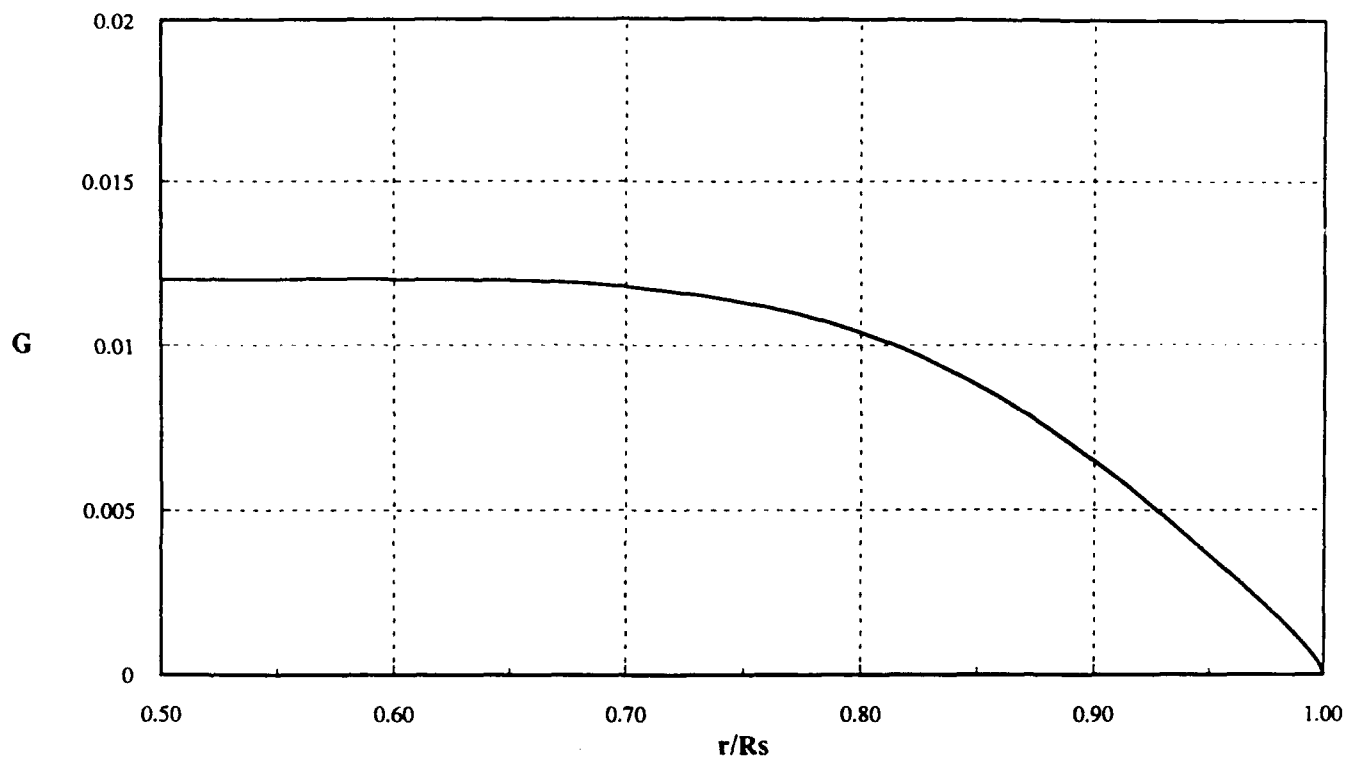


Figure 10. Stator Design Load Distribution

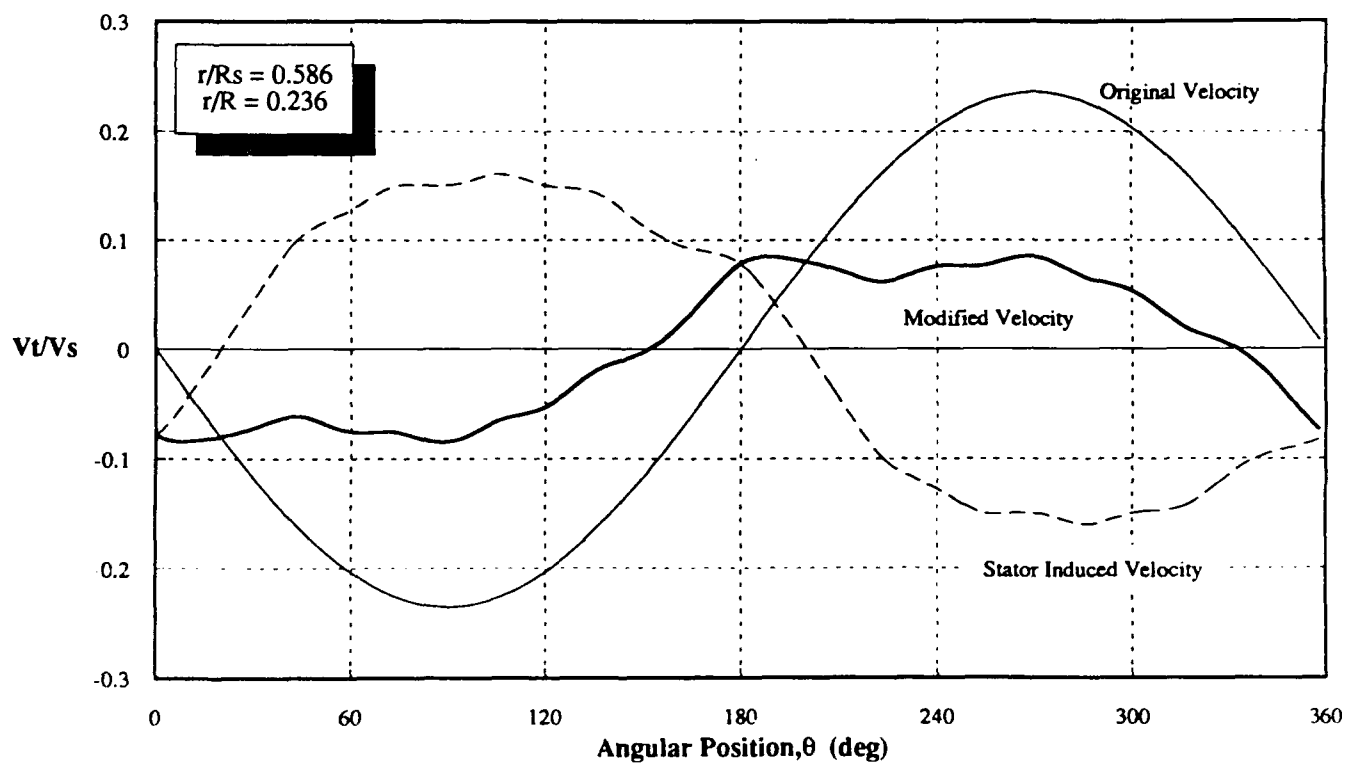


Figure 11a. Propeller Radius = 0.236R

Figure 11. Modified Tangential Wake in the Propeller Plane

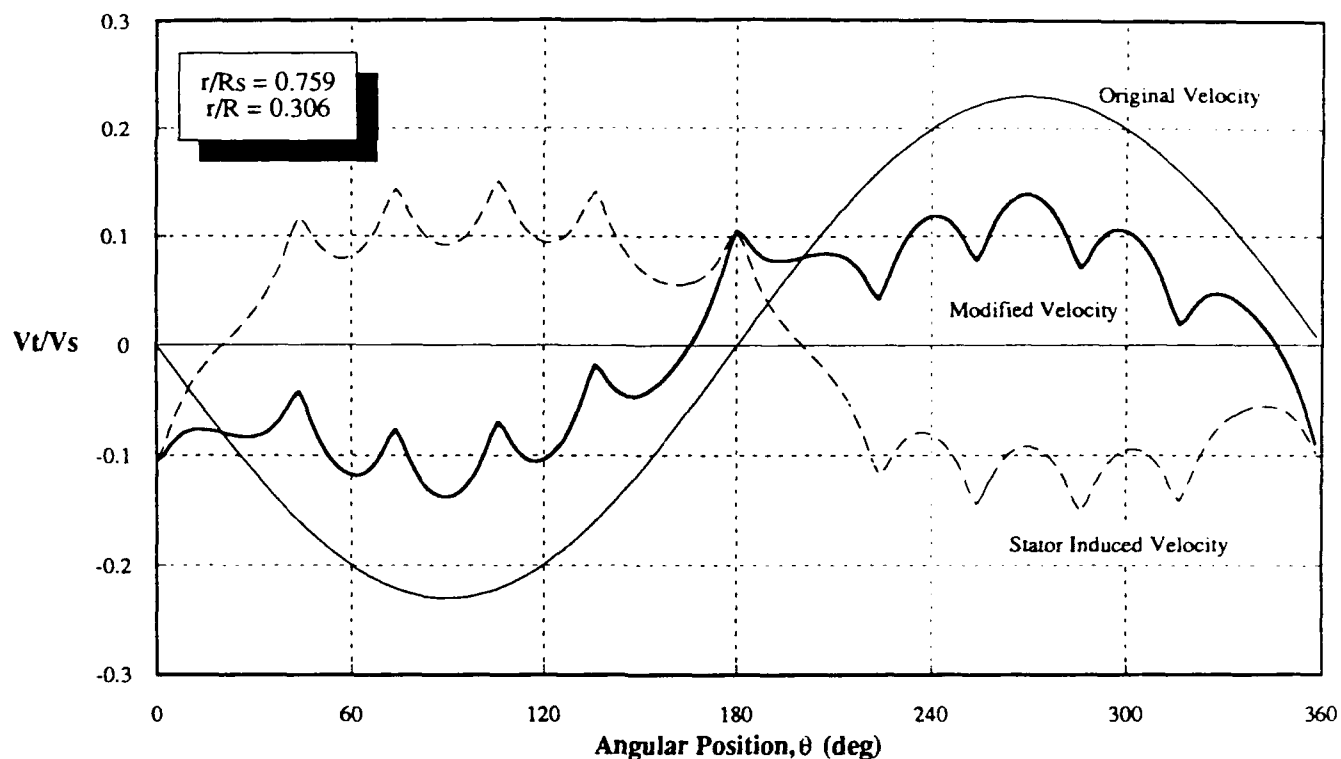


Figure 11b. Propeller Radius = $0.306R$

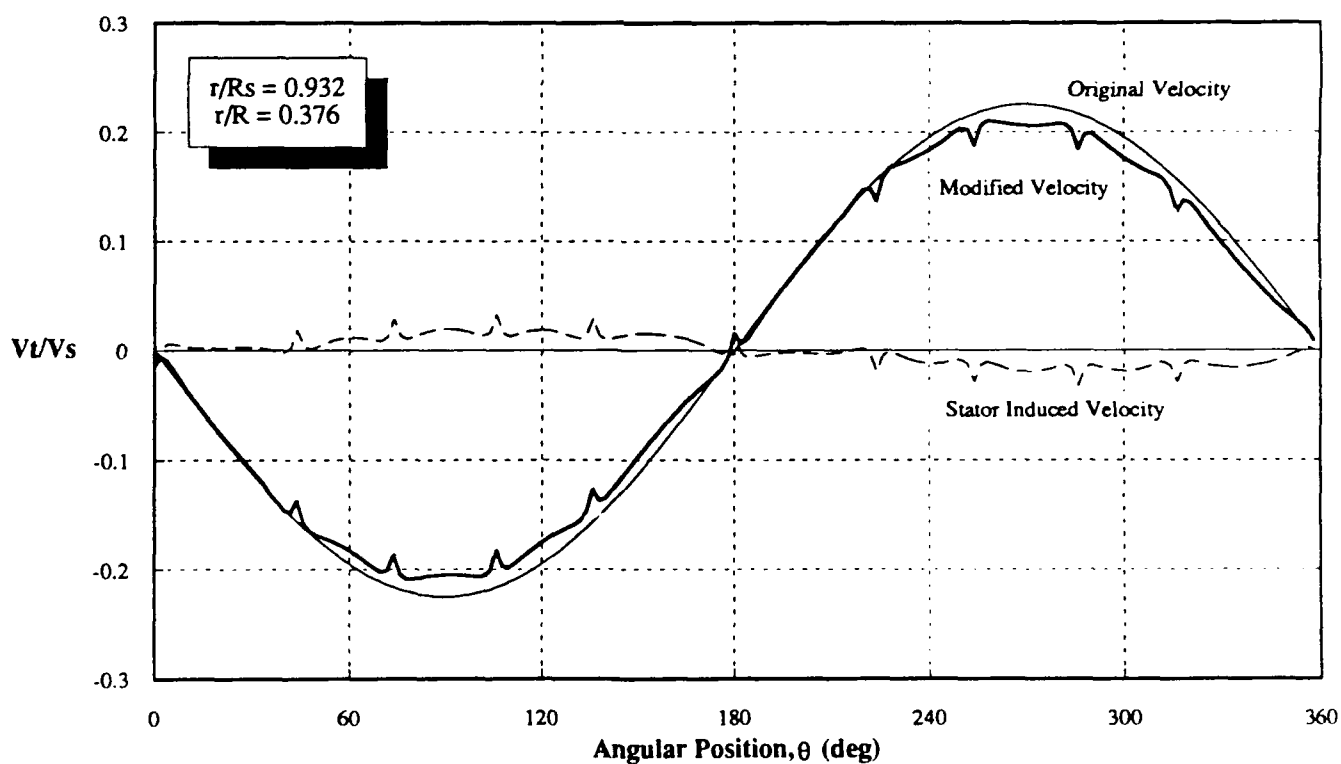


Figure 11c. Propeller Radius = $0.376R$

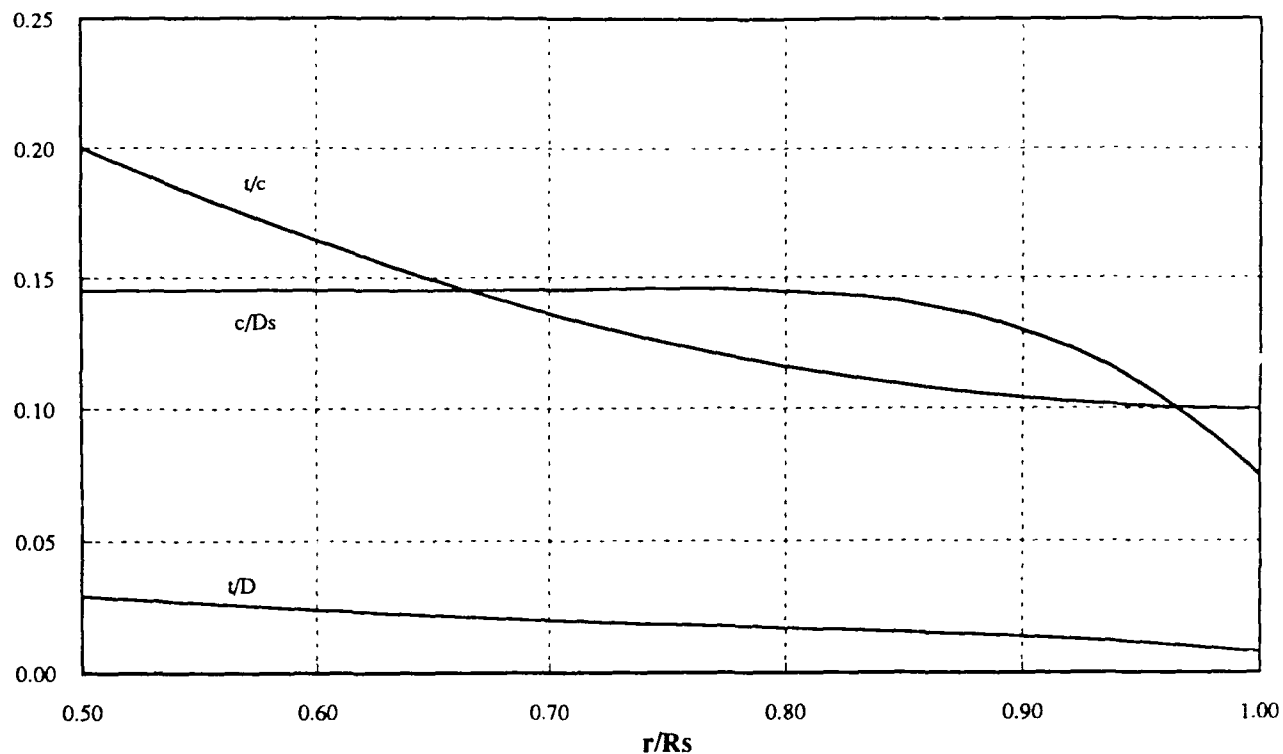


Figure 12. Stator Chord and Thickness

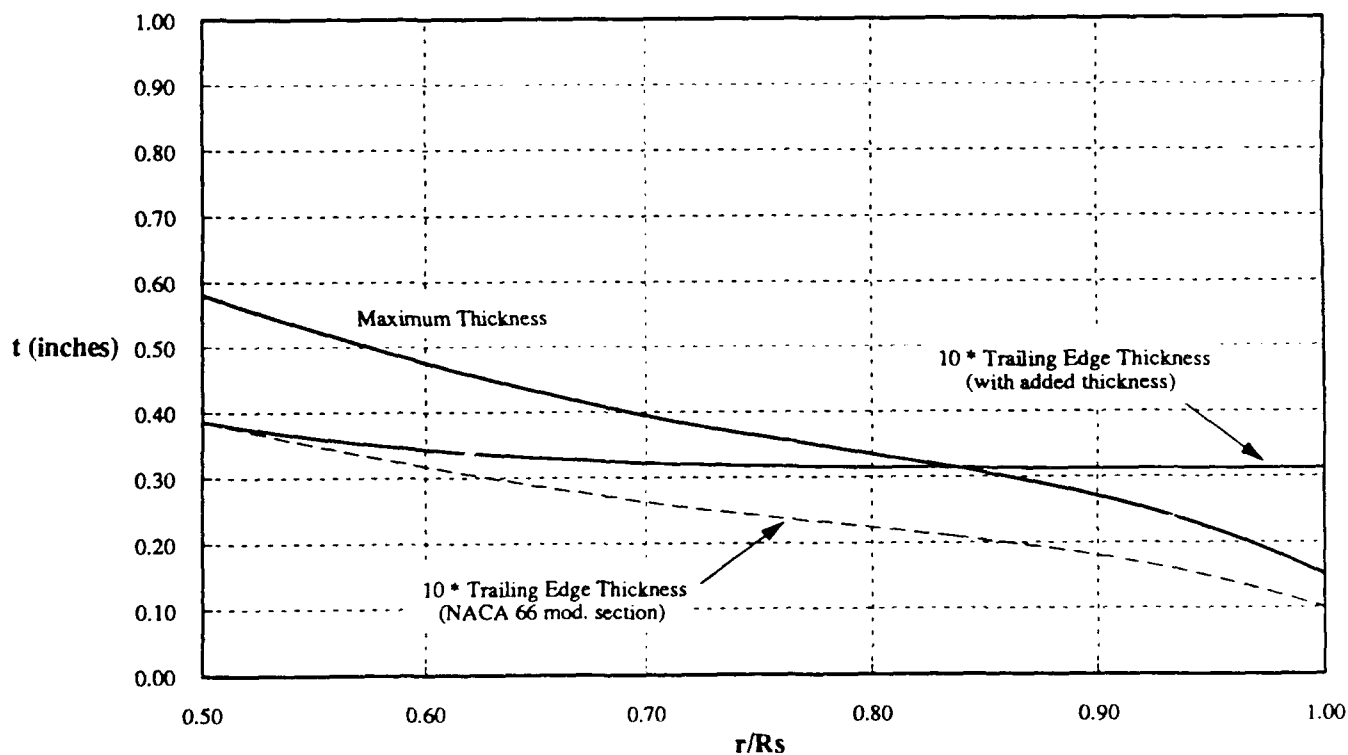


Figure 13. Section Maximum Thickness and Trailing Edge Thickness

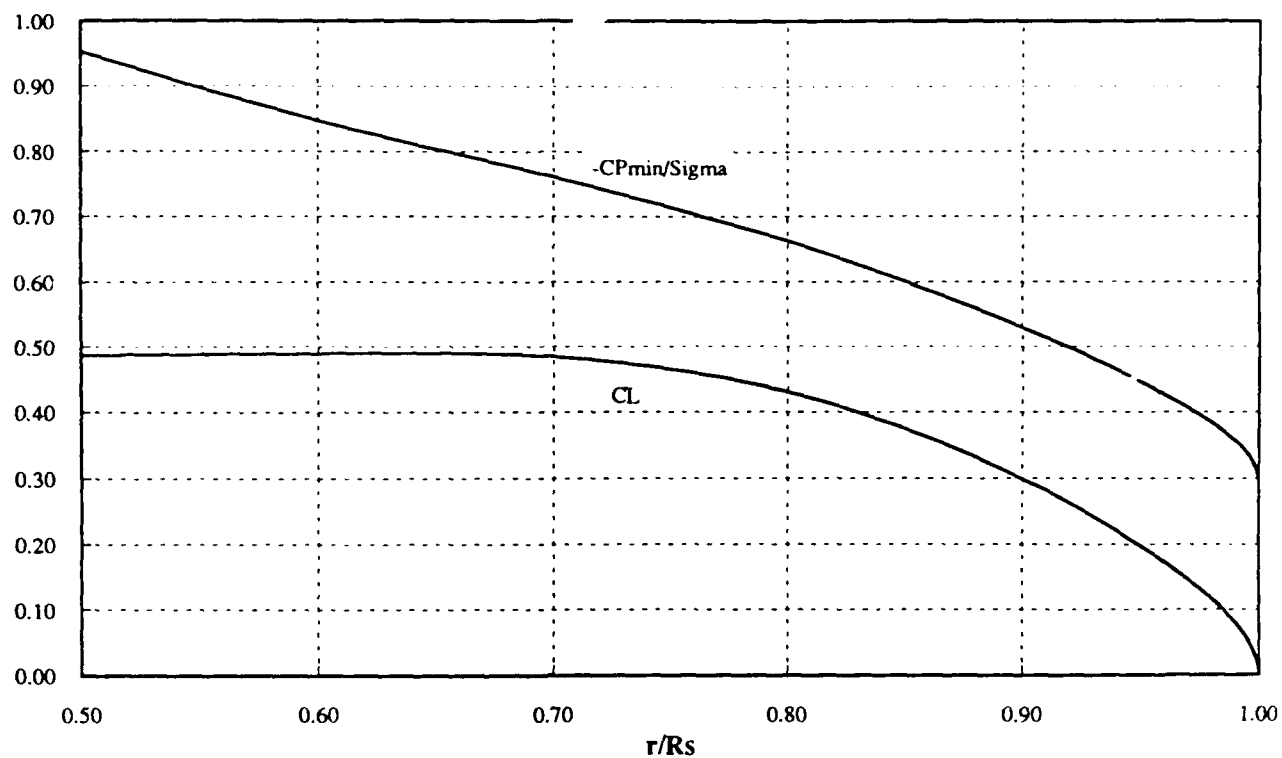


Figure 14a. Lift Coefficient and Back Bubble Cavitation Margin

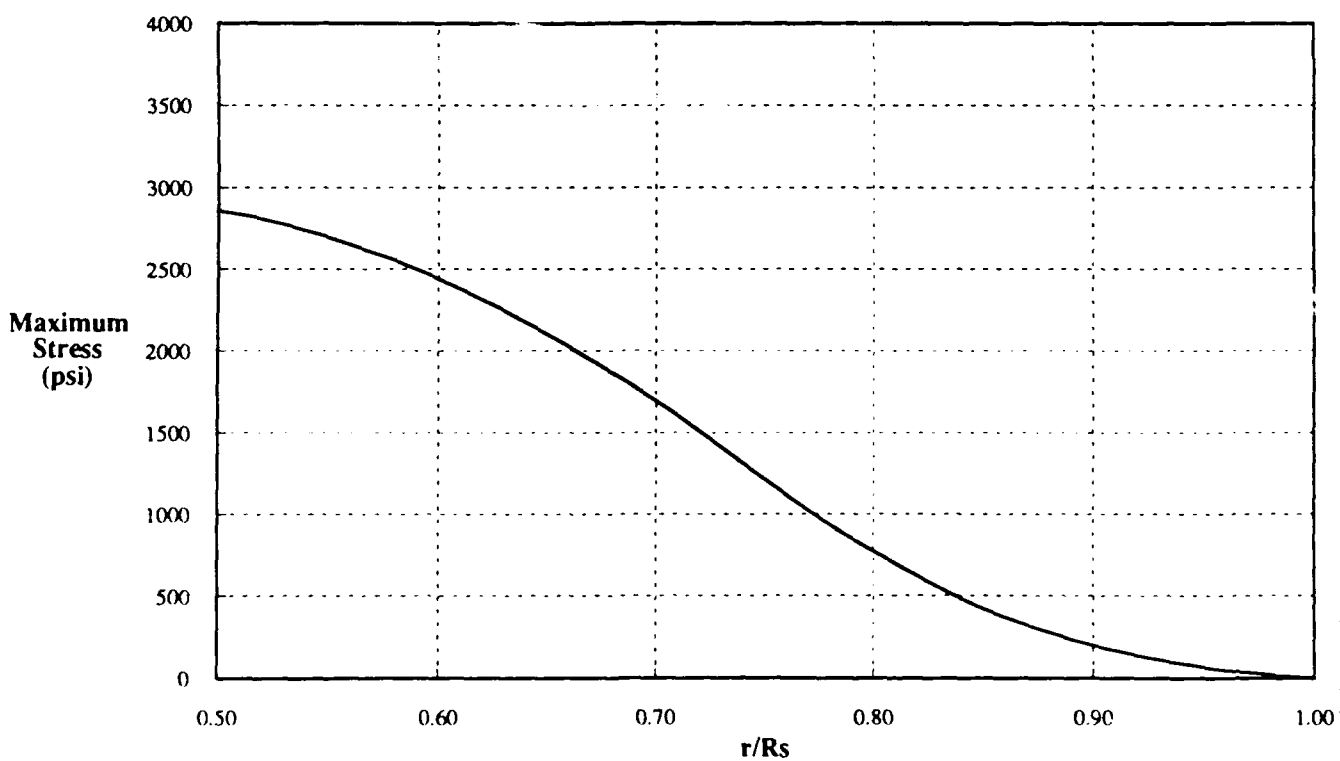


Figure 14b. Maximum Stress (30 kts)

Figure 14. Stator Design Parameters

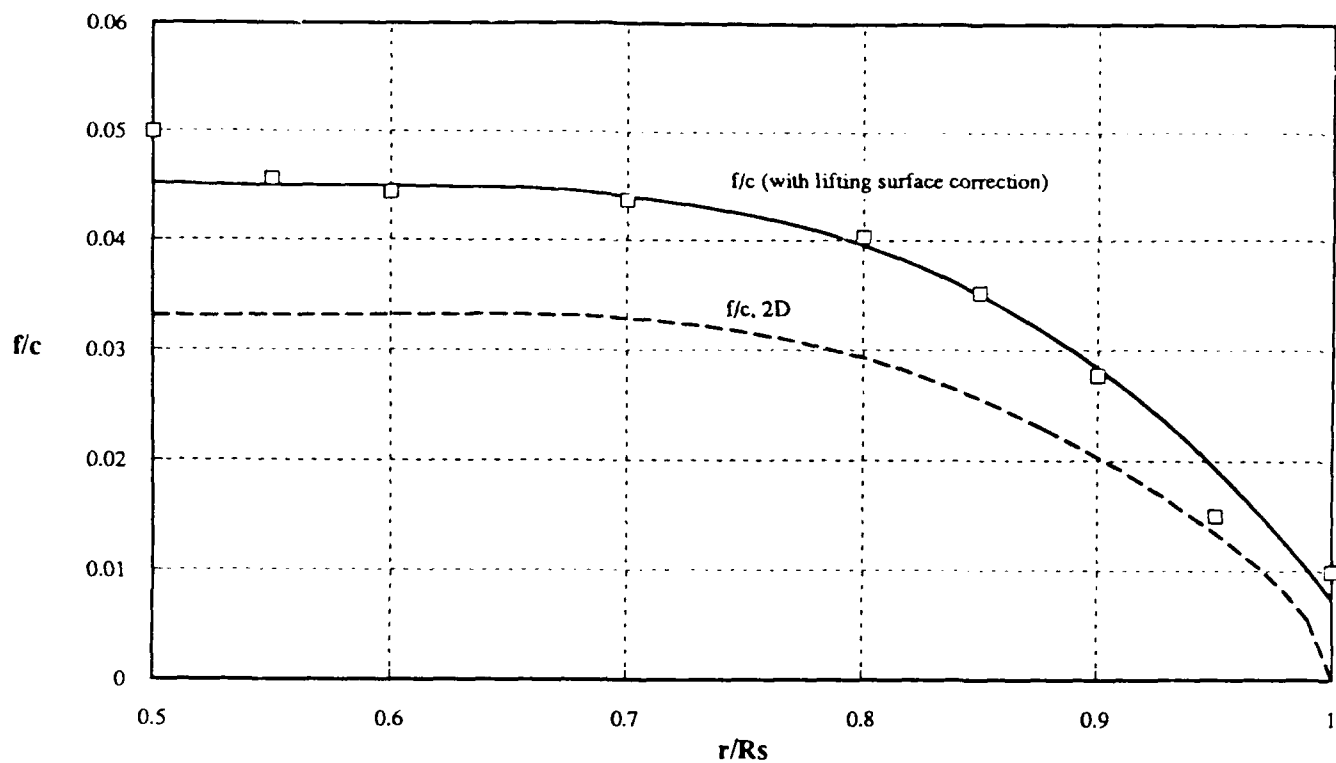


Figure 15. Stator Camber Distribution

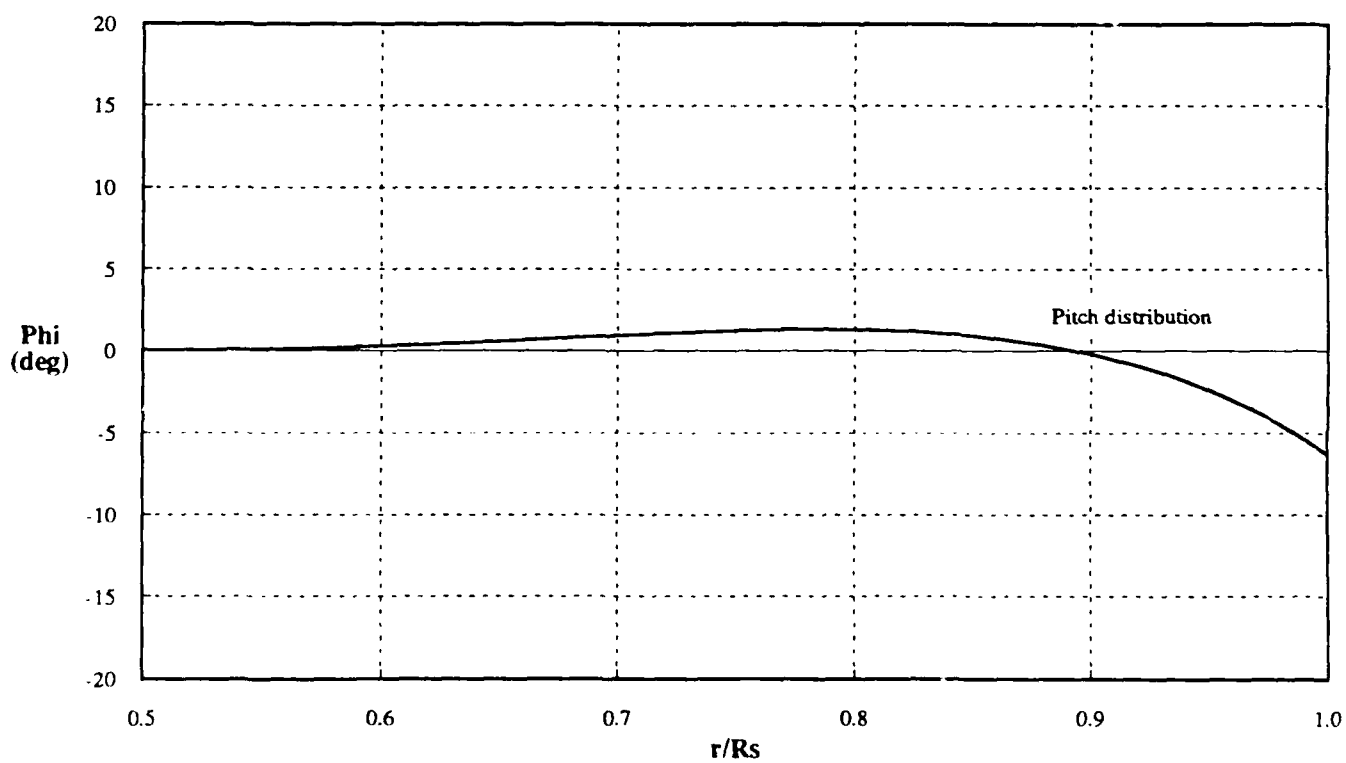


Figure 16. Stator Pitch Distribution

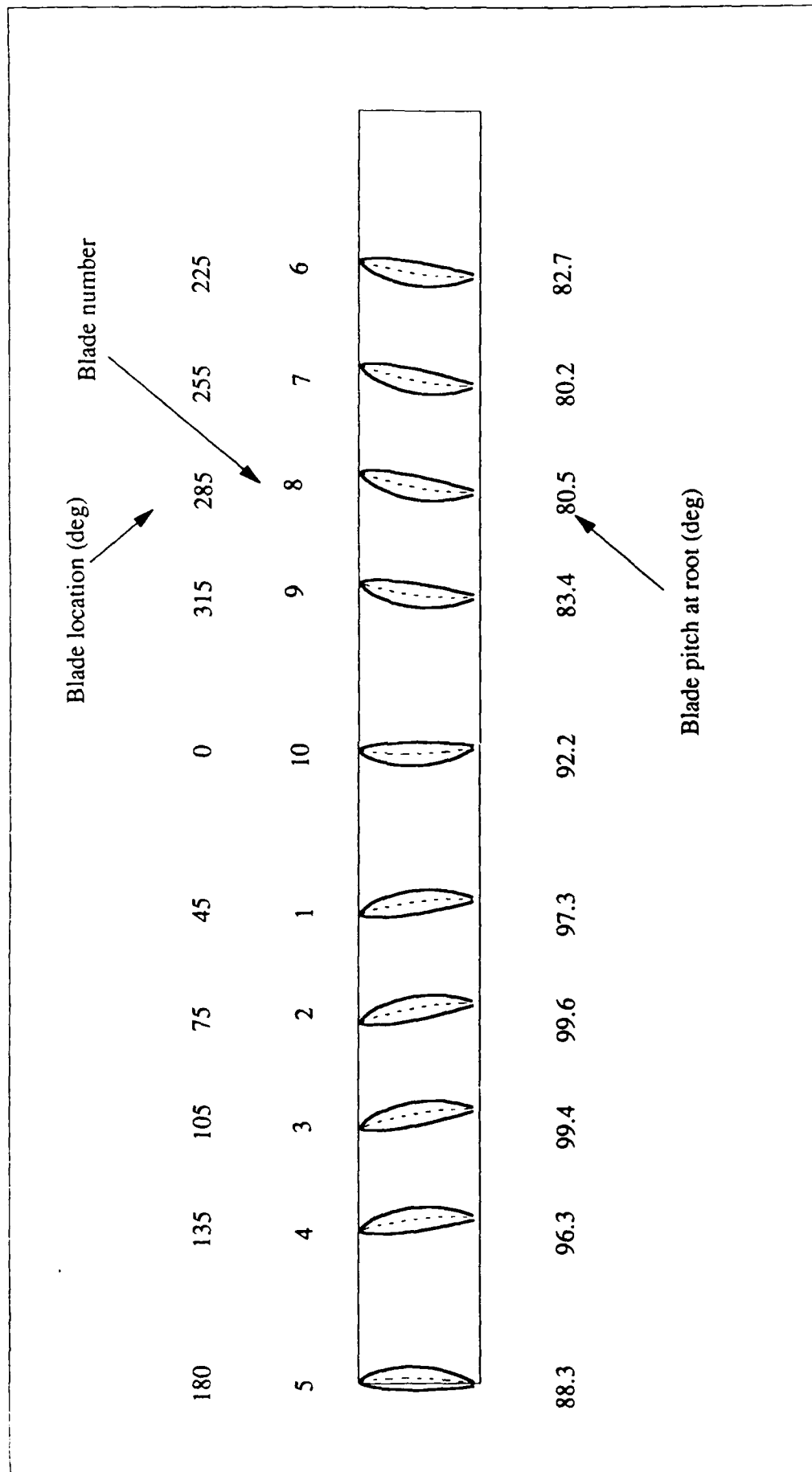


Figure 17. Expanded Hub

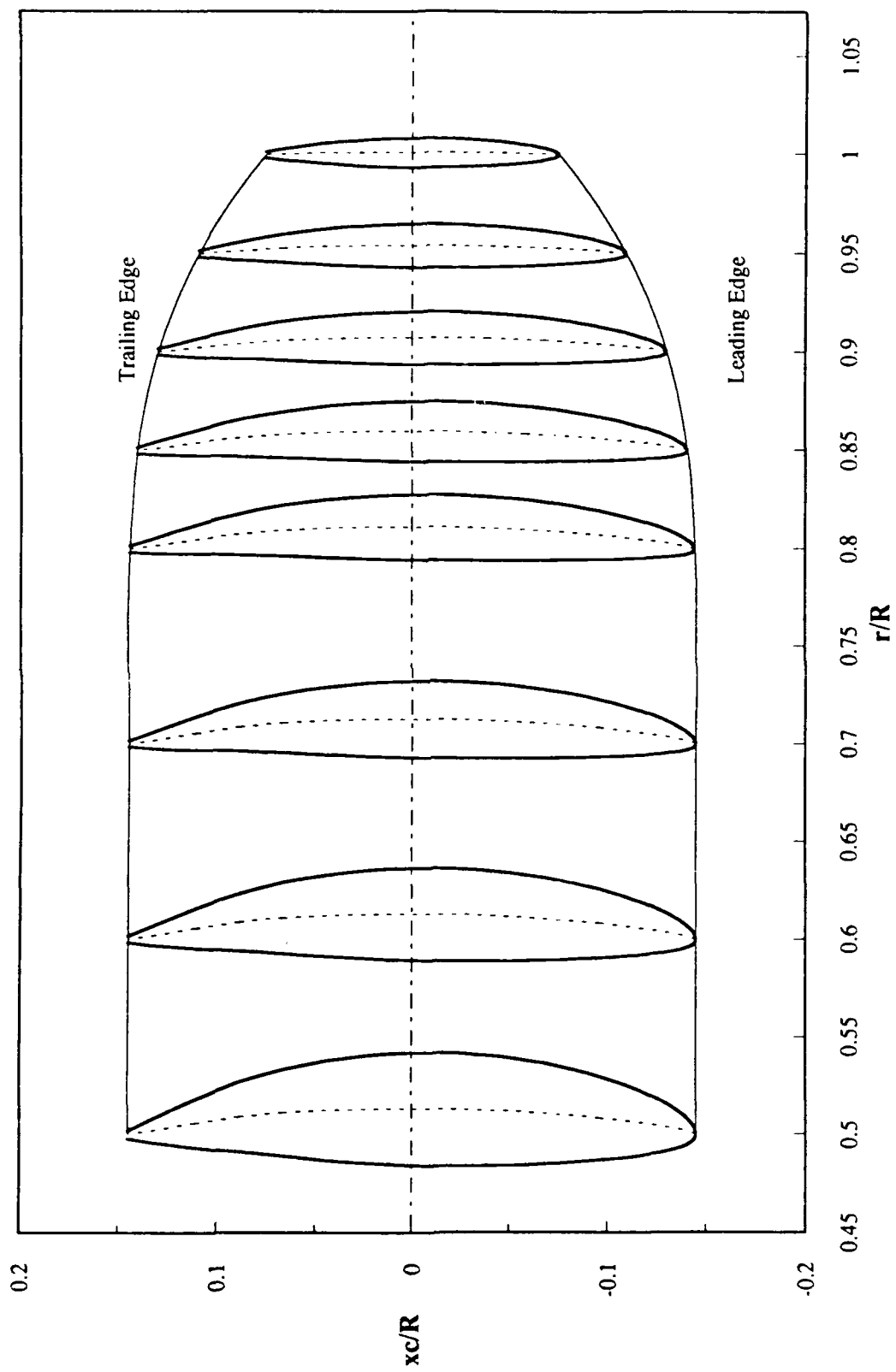


Figure 18. Stator Blade Sections

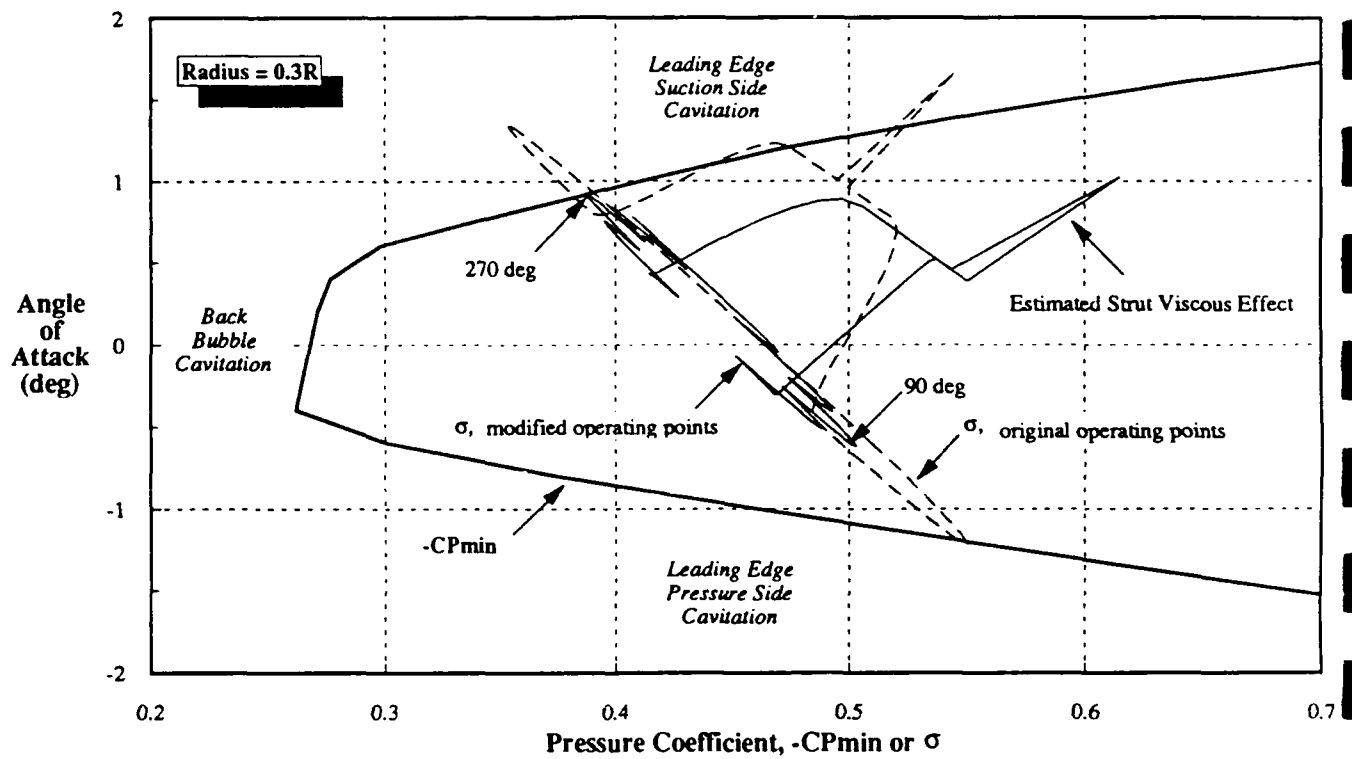


Figure 19. Cavitation Bucket with Modified Inflow -- $0.3R$

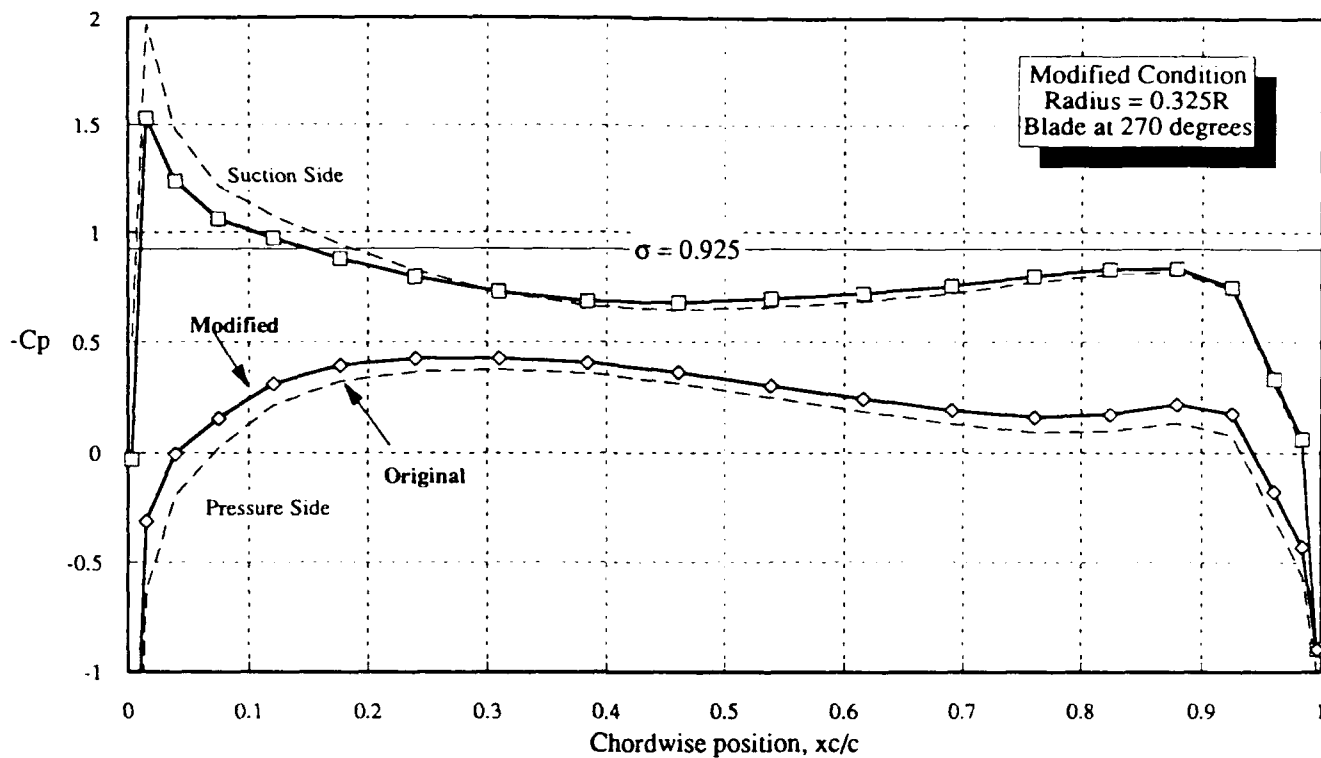


Figure 20a. Blade at 270 degrees

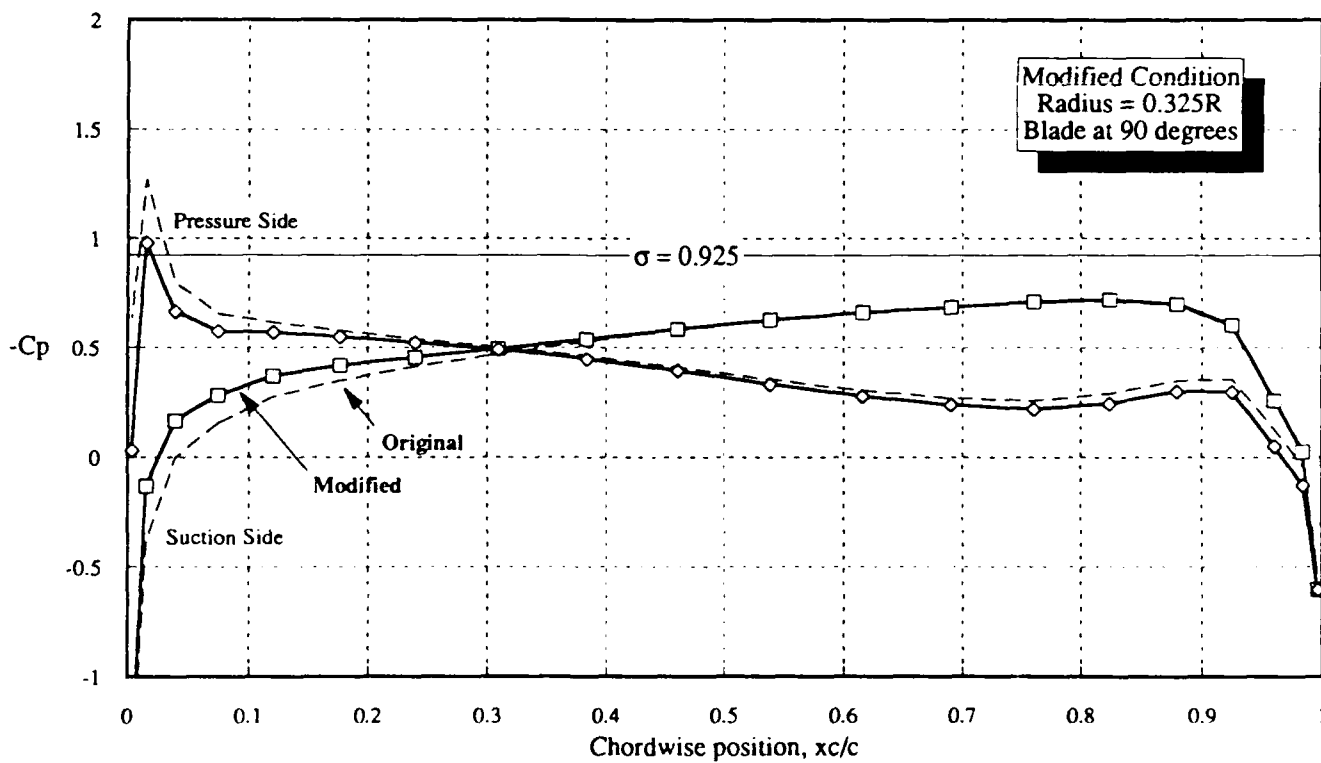


Figure 20b. Blade at 90 degrees

Figure 20. Modified Chordwise Pressure Distribution -- 0.325R

Table 1. Stator Design Geometry
($D=20$ in.)

r/R	c/D	t/c	t/D	t_{TE}/t	f/c	ϕ (deg)	θ_S (deg)	x_R/D
0.50	0.1450	0.2000	0.02900	0.0667	0.04518	0.00	0.00	0.00
0.55	0.1450	0.1810	0.02625	0.0688	0.04494	0.07	0.00	0.00
0.60	0.1450	0.1640	0.02378	0.0721	0.04492	0.27	0.00	0.00
0.70	0.1450	0.1360	0.01972	0.0817	0.04406	0.94	0.00	0.00
0.80	0.1444	0.1160	0.01675	0.0938	0.03957	1.31	0.00	0.00
0.85	0.1405	0.1090	0.01531	0.1022	0.03500	0.93	0.00	0.00
0.90	0.1299	0.1040	0.01351	0.1157	0.02838	-0.19	0.00	0.00
0.95	0.1092	0.1010	0.01103	0.1417	0.01932	-2.44	0.00	0.00
1.00	0.0750	0.1000	0.00750	0.2083	0.00745	-6.28	0.00	0.00

(distribution)

Thickness Form: NACA 66 (TMB Modified)
Mean Line: NACA a=0.8

Note:

A parabolic thickness addition is applied from midchord to TE to obtain trailing edge thickness, t_{TE} .
Edge details and fillet are not shown.
Blades 1-5 are "left-handed" and blades 6-10 are "right-handed."
Pitch is adjusted for each blade to obtain root pitch shown in Table 3.

Table 2. Stator Design Geometry (in inches)

r/R	r	c	t	t_{TE}	f
0.50	5.000	2.900	0.580	0.039	0.131
0.55	5.500	2.900	0.525	0.036	0.130
0.60	6.000	2.900	0.476	0.034	0.130
0.70	7.000	2.900	0.394	0.032	0.128
0.80	8.000	2.888	0.335	0.031	0.114
0.85	8.500	2.810	0.306	0.031	0.098
0.90	9.000	2.598	0.270	0.031	0.074
0.95	9.500	2.184	0.221	0.031	0.042
1.00	10.00	1.500	0.150	0.031	0.011

Note:

A parabolic thickness addition is applied from midchord to TE to obtain trailing edge thickness, t_{TE} .

Edge details and fillet are not shown.

Blades 1-5 are "left-handed" and blades 6-10 are "right-handed."

Table 3. Blade Pitch Settings

Blade Number	Blade Location (deg)	Root Pitch (deg)
1	315	97.3
2	285	99.6
3	255	99.4
4	225	96.3
5	180	88.3
6	135	82.7
7	105	80.2
8	75	80.5
9	45	83.4
10	0	92.2

Note: Pitch is defined as a right hand propeller.

Table 4. Net Stator Forces (per shaft)

Longitudinal:	-11 lbs. (drag)
Vertical:	746 lbs.
Lateral:	224 lbs.

Table 5. Cavitation Inception Speeds (knots)

Prediction Method	Cavitation Type	Original	Modified	Delta
Cavitation buckets	Leading edge suction side:	24.6	30.0	5.4
	Leading edge pressure side:	30.0	38.1	8.1
	Back Bubble:	37.5	36.8	-0.7
Panel code	Leading edge suction side:	22.0	25.6	3.6
	Leading edge pressure side:	24.0	28.0	4.0

REFERENCES

1. Hurwitz, R.B., and L.B. Crook, "Analysis of Wake Survey Experimental Data for Model 5365 Representing the R/V Athena in the DTNSRDC Towing Tank," David Taylor Research Center, Ship Performance Department, Report DTNSRDC/SPD-0833-04, October 1980.
2. Crook, L.B., "Powering Predictions for the R/V Athena (PG 94) Represented by Model 4950-1 with Design Propellers 4710 and 4711," David Taylor Research Center, Ship Performance Department, Report DTNSRDC/SPD-0833-05, January 1981.
3. Greeley, D.S., and J.E. Kerwin, "Numerical Methods for Propeller Design and Analysis in Steady Flow," SNAME Transactions, Vol. 90, 1982.
4. Spangler, P.K., "U.S. Coast Guard 110 ft WPB Island Class Lead Ship Final Documentation Trial Results, WPB 1301-1316, Lead Ship: Edisto (WPB-1313)," Naval Sea Combat Systems Engineering Station Report 60-193, May 1988.
5. Brockett, T., "Minimum Pressure Envelopes for Modified NACA-66 Sections with NACA $a=0.8$ Camber and BUSHIPS Type I and II Sections," David Taylor Research Center, Report 1780, February 1966.
6. Lee, J-T., "A Potential Based Panel Method for the Analysis of Marine Propellers in Steady Flow," Massachusetts Institute of Technology, Department of Ocean Engineering, Report 87-13, 1987.
7. Kerwin, J.E., W.B. Coney, and C-Y. Hsin, "Optimum Circulation Distributions for Single and Multi-Component Propulsors," Twenty-First American Towing Tank Conference, National Academy Press, 1986.
8. Wang, M.H., "Hub Effects in Propeller Design and Analysis," Massachusetts Institute of Technology, Department of Ocean Engineering, Report 85-14, 1985.
9. Hsin, C-Y., "Analysis of the Performance of a Non-Axisymmetric Stator by Lifting Surface Theory," Massachusetts Institute of Technology, Department of Ocean Engineering, 1987.

INITIAL DISTRIBUTION

Copies		1	1521	W. Day
		1	1521	G. Karafiath
2	ARL/PSU			
1	M. Billet	1	1522	D. Jenkins
1	W. Gearhart	1	1522	K. Remmers
		1	1522	T. Smith
2	Bird-Johnson Co.	1	1522	M. Wilson
1	J. Norton			
1	G. Platzer	1	154	J. McCarthy
12	DTIC	1	1542	F. Noblesse
1	MARAD A. Landsburg	15	1544	S. Neely
12	NAVSEA			
1	5112			
1	503			R. Staiman
1	5011			G. Broome
1	55N			R. Biancardi
1	55W32			J. Pattison
1	56X1			J. Dunne
2	56X7			C. Crockett
1	PMS 312A			
1	PMS 330			M. Finnerty
1	PMS 400C			
1	PMS 400D			
1	NOSC 634			T. Mautner
1	NRL 1006			
1	NUSC 01V			
5	US Coast Guard (RD&C)			
	E. Purcell			

CENTER DISTRIBUTION

Copies	Code	Name
1	1501	D. Goldstein
11	1504	
1	1506	D. Walden
1	1508	R. Boswell
1	1508	W. Cave
1	1509	B. Raver
1	152	W.-C. Lin